Curved nanostructured materials

New Journal of Physics
An Institute of Physics and Deutsche Physikalische Gesellschaft Journal

Curved nanostructured materials

Humberto Terrones and Mauricio Terrones
Advanced Materials Department, IPICyT, Camino a la Presa San José 2055, 78216 San Luis Potosí, SLP, Mexico
E-mail: hterrones@ipicyt.edu.mx and mterrones@ipicyt.edu.mx

New Journal of Physics **5** (2003) 126.1–126.37 (http://www.njp.org/)
Received 7 July 2003
Published 3 October 2003

Abstract. Graphite is a layered material that is very flexible, in which each layer is able to curve in order to form cages, nanotubes, nanocoils, nanocones, etc. In this paper, we demonstrate that various synthetic routes are capable of producing graphite-like nanomaterials with fascinating electronic and mechanical properties. There are other layered systems, which could curl and bend, thus generating novel nanostructures with positive and negative Gaussian curvature. In this context, we will also demonstrate that hexagonal boron nitride, tungsten disulfide (WS_2), molybdenum disulfide (MoS_2) and rhenium disulfide (ReS_2) are also able to create nanocages, nanotubes and nano-arrangements exhibiting novel physico-chemical properties that could revolutionize materials science in the 21st century.

Contents

PII: S1367-2630(03)65766-6

1. Introduction

Layered materials, consisting of atoms arranged in a layer-by-layer fashion, are abundant in nature. Graphite is a clear example of such a material, in which sp^2 hybridized carbon atoms are arranged in a hexagonal lattice and every carbon is bonded to three others (figures 1(a) and (b)). Interestingly, carbon is also able to form diamond, where carbon atoms are surrounded by four atoms placed at the vertices of a tetrahedron (figure 1(c)). The different electronic and mechanical properties observed for graphite and diamond are caused by their bonding nature and crystal structure: graphite is a semimetal, whereas diamond is an insulator; graphite is soft and diamond is one of the hardest materials ever observed. Although graphite is 'soft', the in-plane carbon–carbon bond of individual layers is extremely strong. In 1985, Kroto and colleagues [1] found that carbon could also form cage-like molecules in which every atom is connected to three neighbours (sp^2 hybridization), as in graphite. These carbon cages were named fullerenes in honor of Richard Buckminsterfuller, an American architect who developed geodesic domes. In particular, the most abundant fullerene molecule is formed with 60 carbon atoms and it is known as C_{60} or Buckminsterfullerene. In 1990 it was proved that C_{60} molecules crystallize forming bulk crystals, now known as fullerite [2]. A year later, Iijima found that graphite is able to roll into cylinders, thus forming carbon nanotubes (CNTs) of different chiralities.

The discovery of fullerenes [1, 2] and the identification of CNTs [3] has triggered new research areas in physics, chemistry and materials science, that have resulted in the observation of new phenomena with important implications in the development of unique technological devices. Examples are: nanoelectronic devices, quantum wires, electron field emitters for ultra-thin TV screens, nanoprobes, high resolution tips for scanning and atomic force microscopes, sensors, ultra-high-strength composites, gas storage nanodevices and parts of nanomachines, among others [4]–[8].

Fullerenes and CNTs consist of closed fragments of graphite. For fullerenes, the graphite curves and closes due to the presence of 12 pentagonal rings within the hexagonal sheet [9, 10]. Nanotubes could be generated either by rolling a graphene sheet so as to form a cylinder [3, 9, 10], or by elongating a fullerene along a preferential axis. In particular, fullerenes and nanotubes could be nested, thus forming onion-like structures [11, 12] and multi-walled CNTs [3].

In 1991, Mackay and Terrones introduced the concept of negative curvature in the context of periodic graphitic structures with the same shapes as triply periodic minimal surfaces (TPMS) [13]. The authors demonstrated that these structures were energetically stable and therefore possible to synthesize. Moreover, they used differential geometry and topology concepts to prove that other layered materials can also acquire different types of curvature, thus producing materials with novel properties. In addition, they also introduced the term 'flexicrystallography', which refers to curved atomic structures [9, 10, 14]. In flexicrystallography, curvature is the key concept in studying new materials. Similar to graphite, there are other layered structures that can be curved, rolled and bent such as hexagonal boron nitride (hBN), tungsten and molybdenum disulfides, etc.

In this paper, we describe the importance of layered nanomaterials for the fabrication of novel nano-technological devices. We will also show experimental and theoretical results on these nanosystems.

2. Graphite and curved surfaces

Graphite is formed by overlapping flat hexagonal layers of carbon atoms separated by 3.35 Å. The C–C distance is 1.42 Å and the structure belongs to the $P63mc$ (no 186) space group with

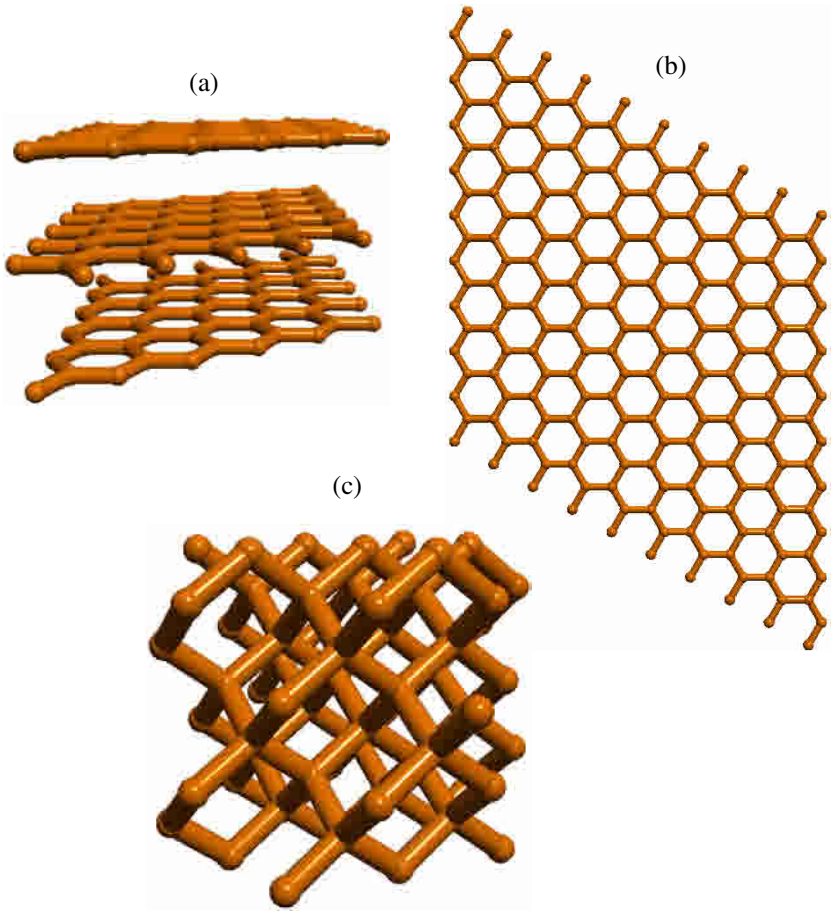

Figure 1. (a) Three graphene sheets separated by 3.35 Å to form graphite, (b) graphene sheet seen from above; note the hexagonal rings of carbon, (c) section of diamond structure.

lattice constants $a = 2.46$ Å and $c = 6.71$ Å, containing two atoms in the asymmetric unit with fractional coordinates (0, 0, 0 and 2/3, 1/3, 1/5; see figure 1).

As mentioned earlier, a key concept in materials is the 'curvature' of the surface. If we consider that graphite and other layered materials form surfaces, then it is possible to define curvature as if the surface was a continuum. A 2D surface embedded in a 3D space exhibits two principal curvatures C_1 and C_2. The product of the two principal curvatures is called the Gaussian 'K' curvature ($K = C_1C_2$) and the average curvature, known as mean curvature, can be expressed as $H = (C_1 + C_2)/2$ [9, 10, 15]. According to the type of Gaussian curvature K, there are three types of geometries in a 3D space [16]:

(a) Euclidean geometry, where K is zero (both principal curvatures are zero);
(b) spherical or ellipsoidal geometry, where $K > 0$ (the surface bends equally at both sides),
(c) hyperbolic geometry, where $K < 0$ (the principal curvatures possess different signs and the surface is composed of saddle points) (figure 2).

These three geometries exhibit different properties. For example: in Euclidean geometry the sum of the interior angles of a triangle is exactly 180°, in spherical geometries this sum is

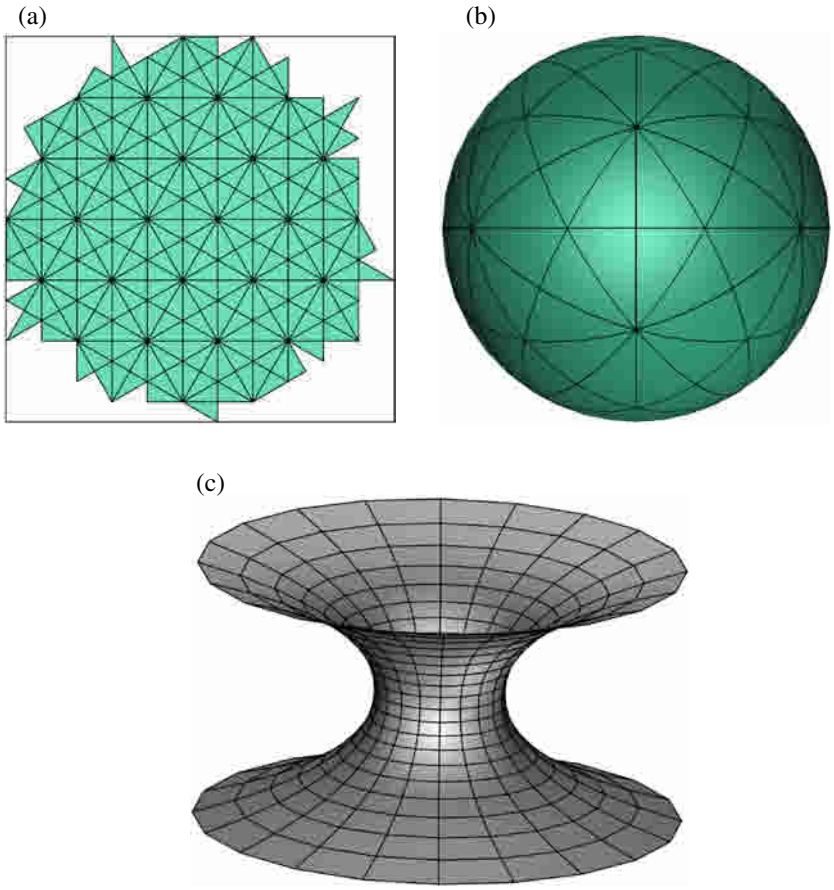

Figure 2. Three 2D geometries in three dimensions. (a) Euclidean geometry $K = 0$ (plane), (b) spherical geometry $K > 0$, (c) a catenoid is an example of hyperbolic geometry in which all points have $K < 0$ (saddle points), where K is the Gaussian curvature.

greater than 180° and in hyperbolic geometries the sum of the interior angles of a triangle is less than 180°. Therefore, the plane is a Euclidean surface, the sphere belongs to spherical geometry and a surface composed of saddle points corresponds to hyperbolic geometry. In nature, there are structures with different levels of complexity and various types of curvature, which are closely related to mathematical complexity (see below).

It is therefore clear that graphite belongs to the Euclidean geometry and C_{60} to the spherical geometry, but these are not all the possibilities. Applying the Gauss–Bonnet theorem to a closed orientable surface, and Euler's law to a graphitic sheet, in which every atom is linked to three others (sp^2 bonding), it is possible to obtain the following relationship:

$$2N_4 + N_5 - N_7 - 2N_8 = 12(1 - g), \tag{1}$$

where N_4, N_5, N_7 and N_8 are the number of squares, pentagonal, heptagonal and octagonal rings of carbon, respectively, and 'g' is the genus of the structure which refers to the complexity of the arrangement. As 'g' increases the complexity also increases. In other words, 'g' is the number of handles or holes in the structure; '$g = 0$' for a sphere, '$g = 1$' for a torus. Note that in the above equation the hexagonal rings are not present: this is because hexagons do not contribute

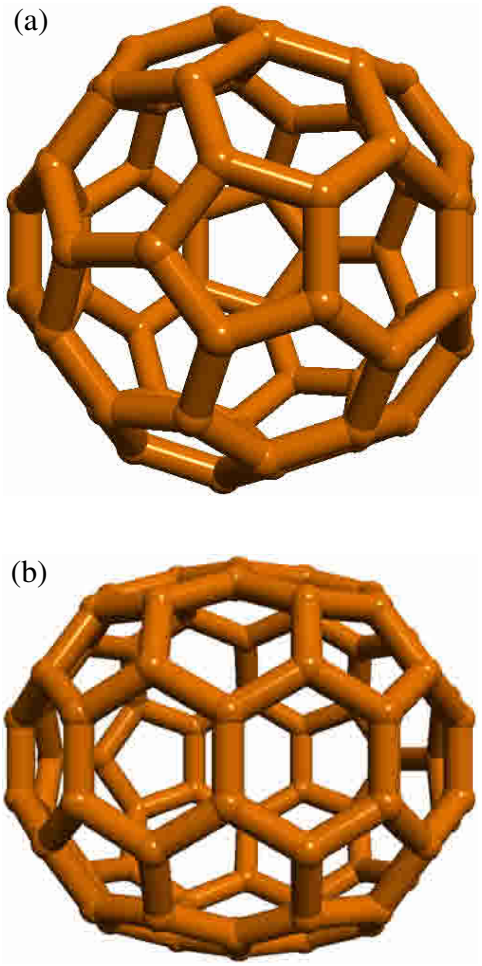

Figure 3. (a) Buckminsterfullerene $C_{60}(I_h)$ composed of 60 carbon atoms. (b) $C_{70}(D_{5h})$ composed of 70 carbon atoms.

to the topology (curvature) of the arrangement. Since C_{60} has the same topology as the sphere, $g = 0$, then $N_5 = 12$ and $N_4 = N_7 = N_8 = 0$. Therefore, there are just 12 pentagons in C_{60} (the same number of pentagons in a soccer ball).

2.1. C_{60} *and other fullerenes*

Kroto, together with his colleagues Curl, Smalley, Heath and O'Brian, carried out experiments consisting of firing a high power laser against a rotating graphite disc under a He atmosphere in order to produce cold carbon clusters. Kroto wanted to simulate the conditions of red giant star formation; these explosions usually produce long carbon chains [17]. Using a time-of-flight mass spectrometer, Kroto and his colleagues identified a large peak commensurate with 60 carbon atoms. After intense discussions and thinking, they concluded that the most stable structure was that of a truncated icosahedron (60 vertices) and decided to call it Buckminsterfullerene or C_{60}. In these experiments, it was also found that there was a smaller peak related to a mass of 70 atoms, which later was identified as another carbon cage molecule consisting of 12 pentagons and 10 additional carbon atoms around the waist of C_{60}. If C_{60} (I_h symmetry) is similar to a soccer ball, C_{70} ($D5_h$ symmetry) is similar to a rugby ball (figure 3).

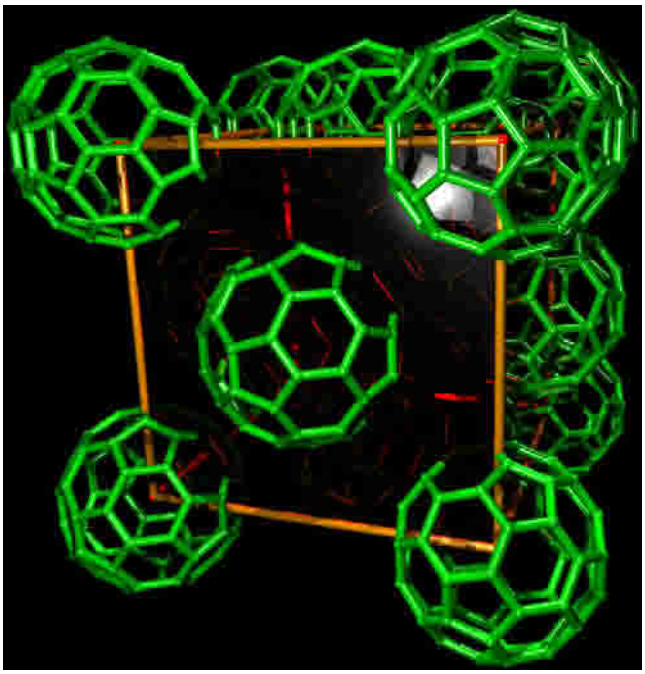

Figure 4. FCC crystal of C_{60} (fullerite).

In 1990 Krätschmer, Huffman and colleagues [2] found that crystals of C_{60} could be produced in macroscopic quantities using an electric arc discharge apparatus. Taylor, Harold Kroto and colleagues [18] also obtained the first NMR spectra of C_{60} and C_{70} and confirmed that the structure of C_{60} was indeed a truncated icosahedron with I_h symmetry (nano-soccer ball). The crystalline structure of solid C_{60} consists of a face centred cubic (FCC) arrangement of C_{60} molecules with a lattice parameter of 14.2 Å (a C_{60} molecule is 7 Å in diameter; figure 4). When these fullerene crystals are doped with alkali metals, such as potassium, caesium or rubidium, it is possible to observe superconductivity as high as 33 K [19, 20]. The insertion of ^{13}C isotopes in C_{60} might shed some light on the vibrational properties of fullerenes [21], and therefore on the superconductivity mechanism.

Kroto generalized the idea of carbon cages and proposed that graphite could produce a whole family of nested cages, now known as giant fullerenes (figure 5). In this context, it is possible to distinguish between classical and non-classical fullerenes: a classical fullerene is a closed carbon cage containing 12 pentagonal rings and any number of hexagons (except one). A non-classical fullerene can admit rings with more that six carbon atoms (heptagons and octagons) and an additional number of pentagons or squares (see the section on graphitic onions).

According to equation (1), it is possible to preserve the genus zero of a fullerene (sphere) by adding rings containing more than six atoms. However additional smaller carbon rings (<6) are necessary to balance this equation and the curvature of the structures. There is experimental evidence that C_{70}, C_{76} [22] and C_{84} [23] also form crystals. In fact, even larger fullerenes exist, but in very small quantities. The most common method used for producing C_{60} is the electric arc discharge of two graphite electrodes [2] (figure 6(a)). In this experiment, the anode is consumed during the reaction, thus forming soot around the chamber; the arc temperatures are around 4200 °C. Alternatively, C_{60} can also be produced via pyrolysis of hydrocarbons in

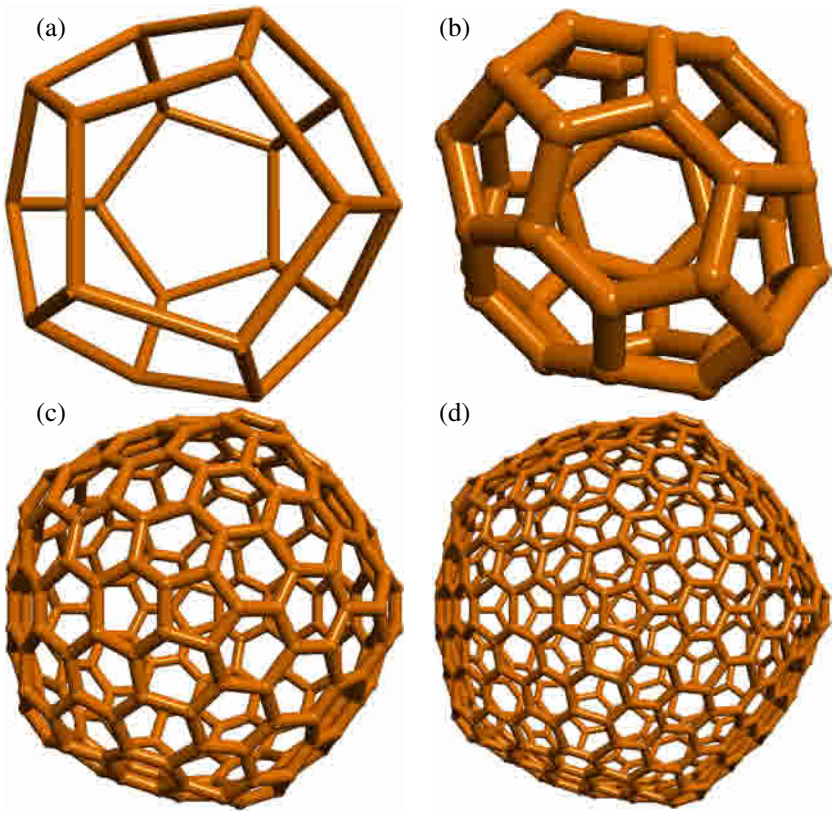

Figure 5. Family of fullerenes. (a) C_{20}, a dodecahedron. (b) C_{40}. (c) C_{240} (icosahedral I_h). (d) C_{540} (icosahedral I_h).

inert atmospheres (naphthalene, coranulene, acetylene, etc) at lower temperatures (e.g. 1000 °C; figure 6(b)).

There are 1812 mathematical ways of forming a closed cage with 60 carbon atoms (isomers), but C_{60} is the most special and stable because all its pentagons are isolated by hexagons. This condition is called the isolated pentagon rule (IPR), which tends to make fullerenes more stable [24]. The next fullerene, which follows the IPR, is C_{70} (it has 8149 possible isomers). Fullerenes with less than 60 atoms cannot have isolated pentagons and therefore they should be highly unstable. Nevertheless, Piskoti *et al* [25] claimed to have synthesized crystals of C_{36}. Unfortunately, the existence of C_{36} has not been fully confirmed to date.

The geometrical construction of a family of chiral fullerenes with icosahedral 'I' symmetry has been proposed by Terrones *et al* [26]. This new type of fullerene is energetically stable and exhibits energies similar to those presented by 'I_h' fullerenes (figure 7). In addition, these structures tend to be metallic.

Other applications of large fullerenes and graphitic polyhedral particles have been proposed for encapsulating different types of elements and compounds in their hollow cavities. In particular, radioactive material can be introduced inside, thus avoiding dangerous leaks [27, 28]. In addition, the role of fullerenes in order to inhibit enzymes related to different viruses has been demonstrated [29, 30].

Regarding the formation of C_{60} two main mechanisms have been proposed: (i) the pentagon road [31] and (ii) the ring road [32, 33]. Recently, Hernández *et al* proposed that non-classical

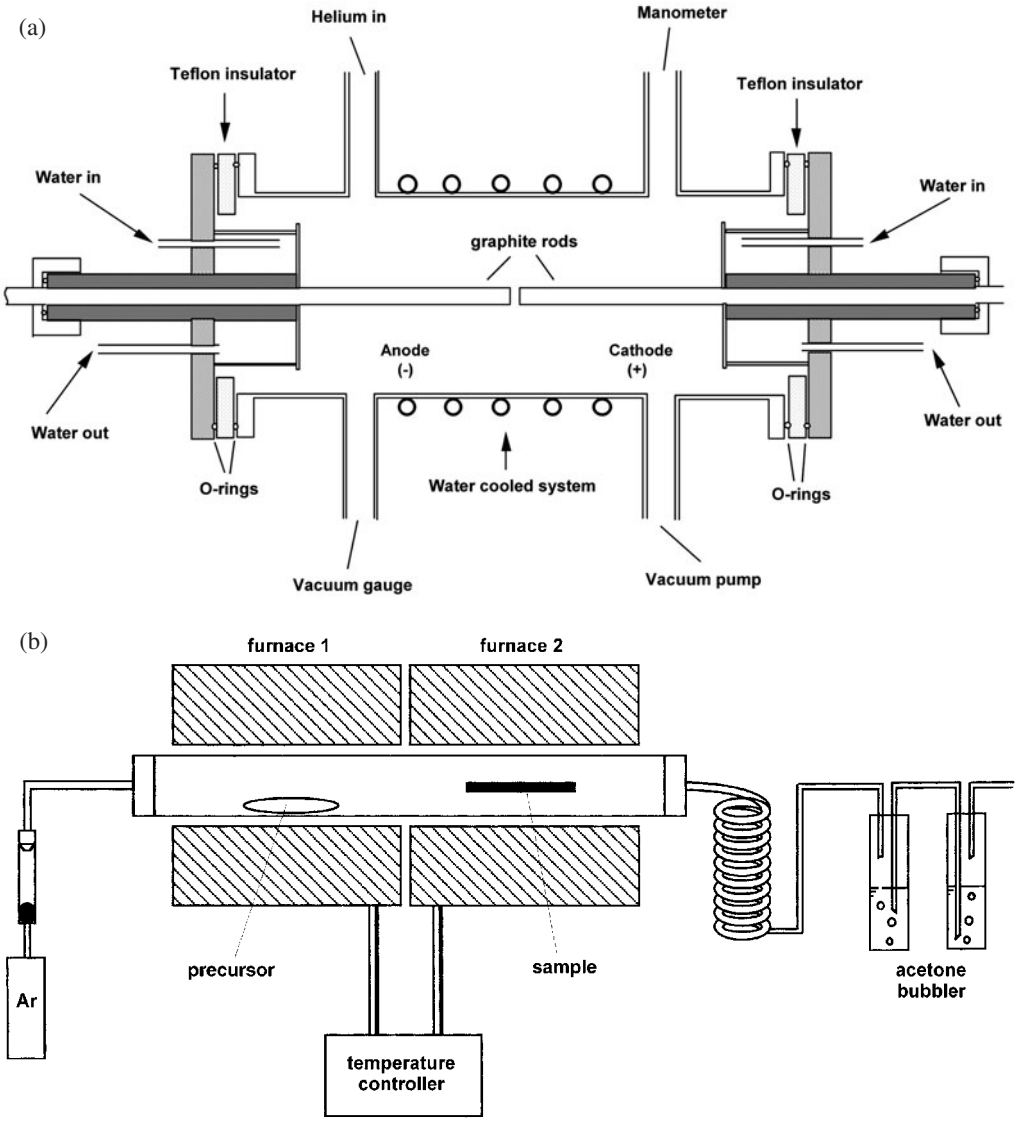

Figure 6. Production methods for fullerenes and CNTs. (a) Arc discharge set-up. (b) Pyrolysis set-up.

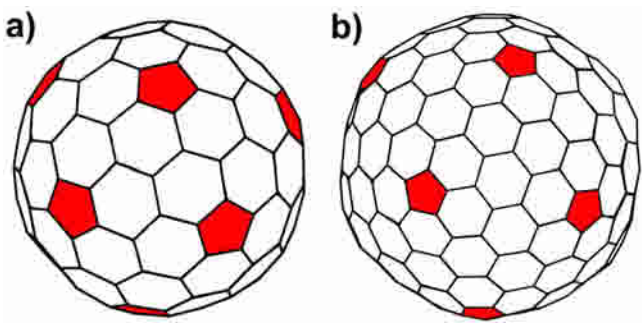

Figure 7. Generated icosahedral (I symmetry) fullerenes with a helical arrangement: (a) C_{140}; (b) C_{260}.

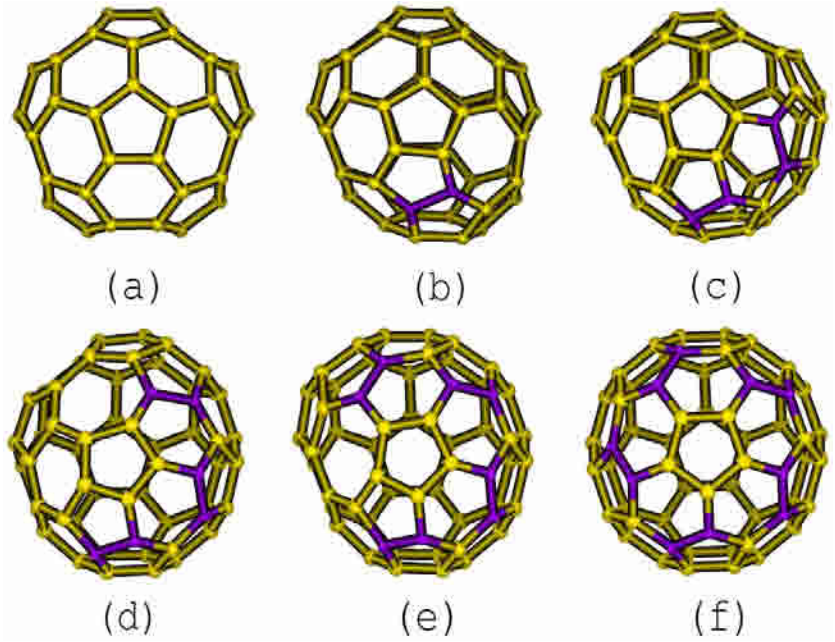

Figure 8. Growing fullerenes through non-classical fullerenes by the dimer addition C_{50} to C_{60} route. (a) $C_{50}(D_{5h})$. (b)–(e) possess one heptagonal ring which rotates around the five-fold axis until reaching C_{60}. (b) C_{52}, (c) C_{54}, (d) C_{56}, (e) C_{58}, (f) C_{60} (I_h, Buckminsterfullerene).

fullerenes, with one heptagonal ring and 13 pentagons, might play an important role in the growing mechanism of C_{60}. The authors found that it is possible to establish routes to grow fullerenes from C_{40} to C_{50} to C_{60} and C_{70} by the addition of carbon dimers to non-classical carbon cages (figure 8) [34]. Unfortunately, no clear experimental evidence for fullerene formation has been reported.

2.2. Onion-like structures

Iijima [35] was the first in recognizing the concentric nature of graphitic polyhedral particles in 1980 using high-resolution transmission electron microscopy (HRTEM). In 1992, Ugarte [11, 12] observed that intense electron irradiation is capable of transforming amorphous carbon and graphitic polyhedral particles into quasi-spherical graphitic nanostructures, known as onion-like particles. These carbon onions can be considered as concentric (nested) arrangements of giant fullerenes, separated by 3.4 Å (the separation between layers in turbostratic graphite). Both Iijima and Ugarte suggested that fullerenes such as C_{60} should be created in the centre of the onions.

It is well known that, as classical fullerenes (12 pentagons only) become larger, the structure becomes more faceted (figure 9) and not spherical like Ugarte's onions. Several groups started to address this problem suggesting the introduction of large carbon rings (heptagons and additional pentagons), so that more spherical structures are created [36]–[38]. In 1997 a mechanism explaining the transformation of polyhedral particles into quasi-spherical graphitic onions was proposed [39]. This mechanism states that fast electrons (from the electron beam generated in the microscope) displace some carbon atoms in the polyhedral particle, thus creating vacancies

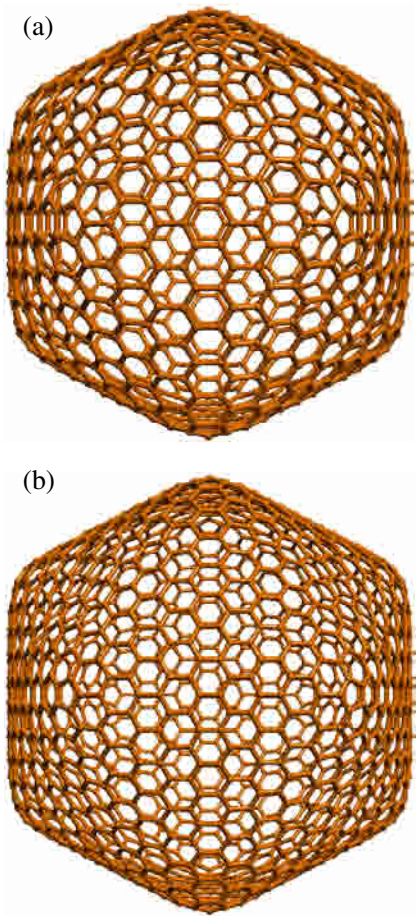

Figure 9. Faceting in giant fullerenes with 12 pentagons. (a) C_{960} (icosahedral, I_h). (b) C_{1500} (icosahedral, I_h). Note how the facing increases as the fullerene grows.

in the strained regions (such as the pentagonal rings). Under these circumstances the structure loses rigidity and starts to reconstruct in order to become stable and spherical. In order to keep the sphericity, the active sites must be satisfied with heptagons and additional pentagons (figure 10). These graphitic onions represent metastable states with fascinating properties. *Ab initio* calculations demonstrated that quasi-spherical onions behave differently electronically when compared to standard icosahedral fullerene cages [40].

It has also been possible to introduce magnetic materials inside carbon onions [41, 42], via thermolytic processes and high electron irradiation [43]. These materials may have important applications in the fabrication of magnetic inks and toners for xerography. More recently, Ajayan and Banhart [43] demonstrated that the internal shells of these onions could be transformed into diamond when high temperatures in conjunction with high electron irradiation are used.

3. Carbon nanotubes

Besides C_{60}, the most studied carbon nanostructure is the nanotube. According to the number of layers, carbon nanotubes can be single-walled carbon nanotubes (SWCNTs) or multi-walled carbon nanotubes (MWCNTs; figure 11). The structure of CNTs were first reported in 1991 by

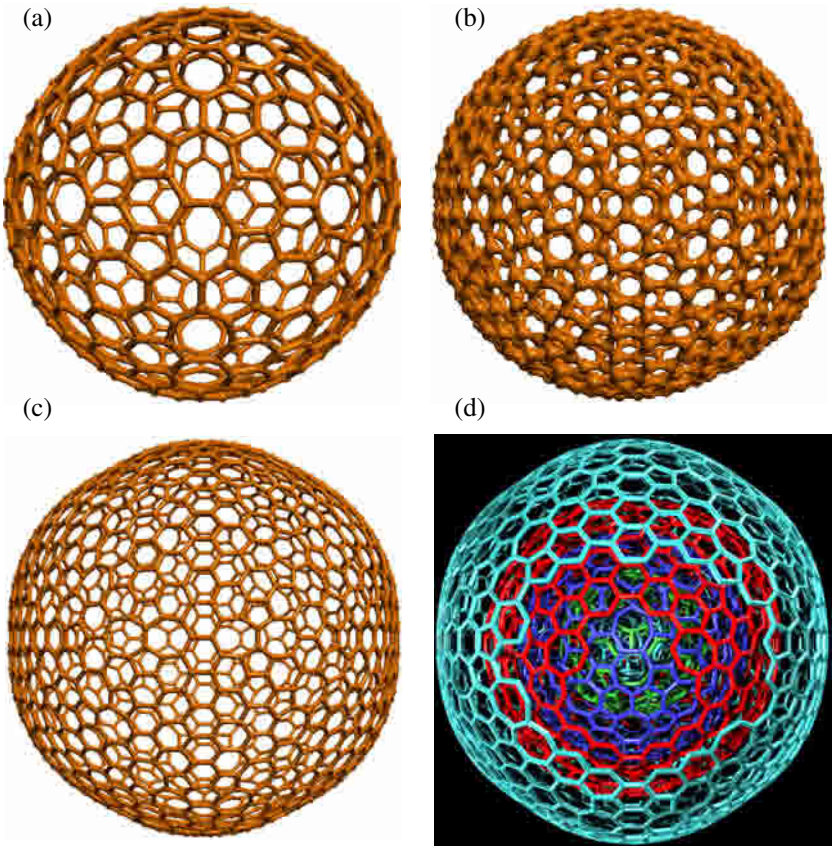

Figure 10. Quasi-spherical fullerenes with heptagons and additional pentagons: 'Terrones model'. (a) C_{540}. (b) C_{960}. (c) C_{1500}. (d) Cut through an onion-like structure made of heptagons, pentagons and hexagons.

Iijima [3]. Iijima realized that graphite could be bent to form MWCNTs with different helicities or chiralities, which refer to the way hexagonal carbon rings are arranged with respect to the tubule axis (figure 12). The structure of CNTs can be characterized using two indices 'm' and 'n': in *armchair* CNTs '$m = n$' (m, m), and in *zigzag* CNT '$n = 0$' $(m, 0)$. In chiral CNTs 'm' and 'n' are different (m, n). Hamada *et al* [44] demonstrated theoretically that the electronic properties of SWCNTs depended on the diameter and chirality: in particular, all of the so-called armchair type nanotubes are electronic conductors (figure 12), whereas zig-zag nanotubes are semiconductors except for the cases in which '$m - n$' is a multiple of 3 (figure 12). Indirect measurements revealed that MWCNTs possess a Young's modulus around 1.8 TPa, which is 100 times larger than that of steel [45]. For this reason, it has been regarded as a structure 100 times stronger than steel and six times lighter (weight-wise). Although composite materials containing CNTs will not be as robust as individual nanotubes, the mechanical properties could be greatly enhanced.

CNTs are produced using four different methods: arc discharge of graphite electrodes in inert atmospheres [3, 46], pyrolysis of hydrocarbons over catalysts [47], laser vaporization of graphite targets [48] and electrolysis of graphite electrodes in molten salts [49, 50]. The arc discharge method (figure 6(a)) is very similar to that used for generating fullerenes [2] with two main differences: first, the inert gas pressures are higher (about 500 Torr of He; for producing

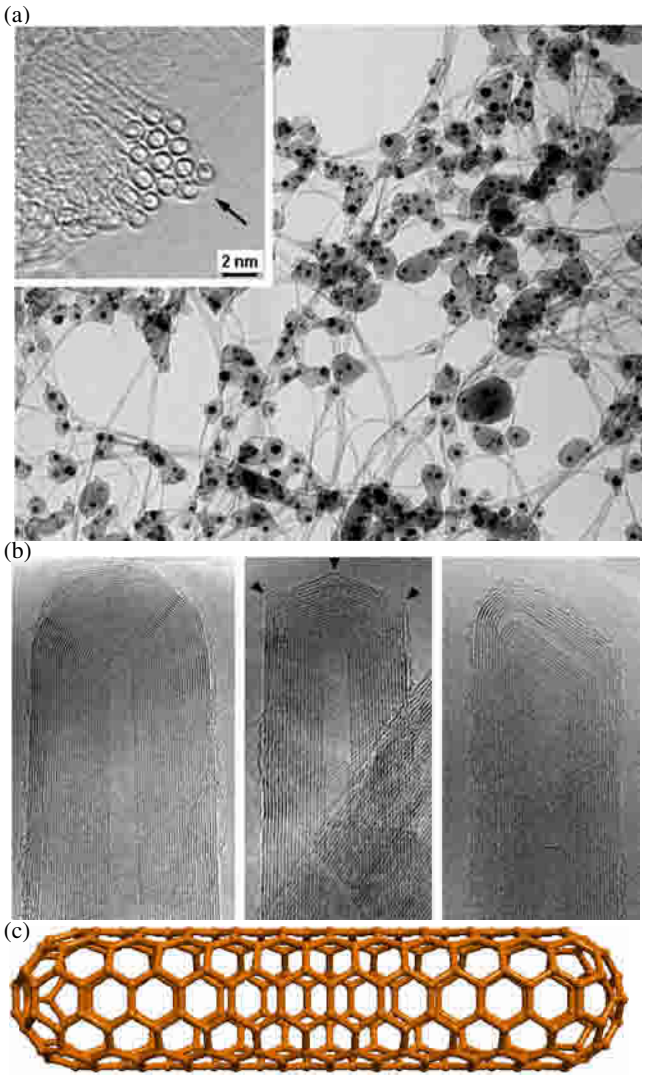

Figure 11. CNTs. (a) Single-walled CNTs obtained with a C/Ni/Y mixture and arc discharge. (b) Tips of multi-walled CNTs. (c) Computer model of a single-walled CNT (elongated fullerene).

fullerenes the pressure is about 100 Torr), and second, the nanotubes grow inside a deposit formed on the cathode, and not in the soot on the walls of the chamber. This method produces highly crystalline MWCNTs with diameters ranging from 2–30 nm. The separation between the cylinders is around 3.4 Å, which is very close to that of graphite (3.35 Å) and corresponds to turbostratic graphite. The lengths of these nanotubes can be up to 30 μm. The optimum conditions for generating nanotubes with this method consist of using currents of 150 A, voltages of 25 V and graphite electrodes between 6 and 8 mm in diameter with a separation between them of 1 mm, always under a helium atmosphere. Unfortunately, the electric arc reaction is too violent, so it is very difficult to control the homogeneity of the tubes (dimensions and shapes).

Two main formation mechanisms have been proposed for arc-grown CNTs: the first establishes that carbon units (C, C_2, C_3, etc) are added to the borders of an open nanotube, thus

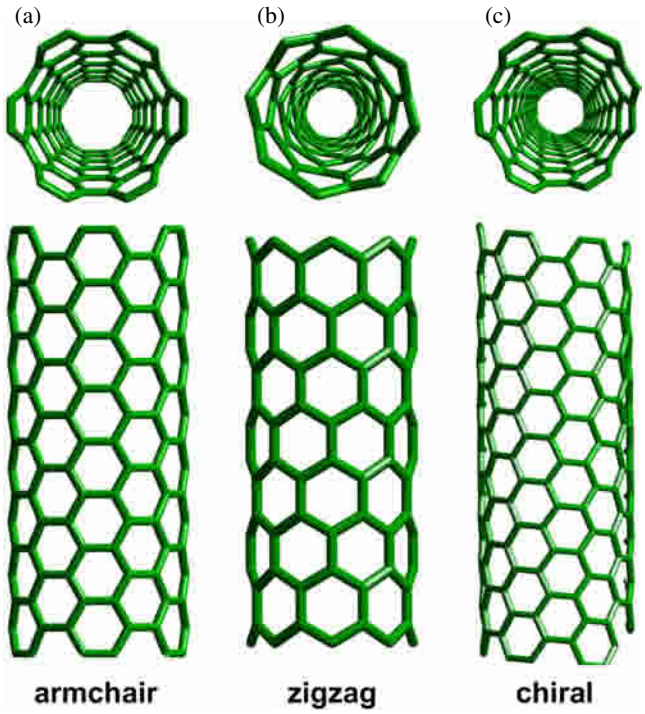

Figure 12. Structures of CNTs: (a) armchair nanotube; (b) zig-zag nanotube; (c) chiral or helical nanotube.

making the tube grow until certain instabilities in the arc produce defects, such as pentagonal rings, causing its closure [51]. The second mechanism proposes that CNTs are elongated fullerenes that grow by the addition of carbon atoms to their surface [52]. It is noteworthy that, besides CNTs, other structures are produced, such as polyhedral particles and amorphous carbon. Therefore, it is important to purify the material obtained by oxidation at high temperatures [46] or by dispersion of colloidal suspensions with surfactants [53, 54]. An analysis of the competition of single- and multi-walled tube formation against fullerenes and onion structures, based on the difference of surface and bond bending energies, has also been reported [55].

With the pyrolysis method it is possible to acquire more control in the CNT formation. This method consists of heating a hydrocarbon or an organic precursor containing carbon in the presence of a metal catalyst (e.g. nickel, cobalt or iron; figure 6(b)). Before the discovery of C_{60}, it was well known that carbon fibres could be obtained by pyrolytic methods using hydrocarbons [56, 57]. In fact, Endo reported the first image of a 4 nm SWNT in the mid-1970s [55]. However, in general, carbon fibres are not nanotubes since the fibres, which usually do not consist of concentric graphene tubes, are larger in diameter and exhibit a great amount of graphitic defects and impurities. Nevertheless, the application of carbon fibres is widespread, showing a mechanical strength comparable to that of steel. According to Dresselhauss *et al* [56] the first record of carbon fibres was realized by Schützenberger and Schützenberger in 1890, more than 100 years ago. Two mechanisms have been proposed for the formation of carbon fibres which can be extended to nanotubes: the first, proposed by Baker *et al*, consists of the diffusion of carbon through the catalytic particle depositing the carbon material on the other side, forming the fibre [56]. The second was proposed by Baird *et al* in 1974 and Oberlin in 1976

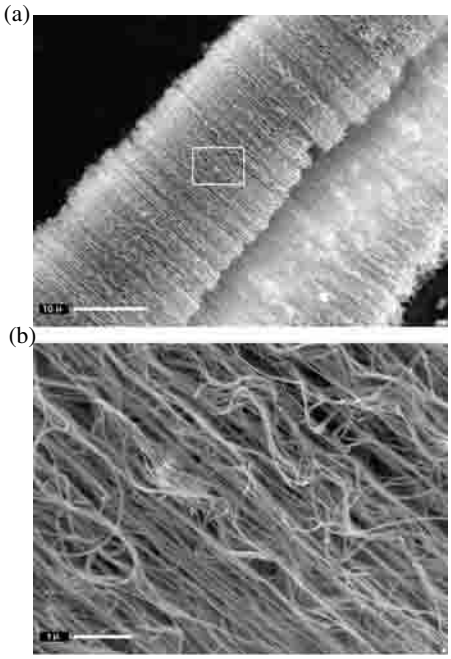

Figure 13. Aligned multi-walled CNTs obtained by laser ablation and pyrolysis.

in which the filaments are formed by diffusion of carbon around the catalytic particle's surface, generating the fibre [56] (chapter 2 of [55] gives a complete account of the synthesis of graphite fibres and filaments). In either of these mechanisms the size of the particle, the nature of the hydrocarbon and the temperature play a crucial role [56, 57].

In 1994, Ajayan and colleagues [58] found that CNTs could be aligned by embedding them in a polymer, thus forming a composite material. When the polymer was cut, the authors observed an aligned arrangement of CNTs. In this context, a better alternative is to use laser ablation of cobalt thin films and then to pyrolyse them with an organic precursor such as 2-amino 4,6-dichloro-S-tryazine [47]. The nanotubes obtained in this way are aligned in bundles which can grow up to 60–100 μm, with diameters between 30 and 50 nm (see figure 13).

The laser vaporization method involves firing a high power laser towards a graphite target inside a furnace at 1200 °C [59, 60]. The condensation of the material generated by the laser is responsible for the nanotube formation. If we add nickel or cobalt to the graphite target, we obtain SWCNTs [48]. They exhibit diameters around 14 Å and form a two-dimensional crystal with a lattice constant of 17 Å. Arrangements of SWCNTs can also be obtained by electric arc discharge when arcing mixtures of carbon, nickel and yttrium [61]–[65].

The electrolysis method is based on using graphite electrodes inside a molten salt such as lithium chloride (700 °C) under an argon atmosphere [49, 50]. Depending on the conditions, up to 20%–30% of the material could consist of MWCNTs. The depth of the cathode and the current (3–10 A) also play an important role in the formation of nanotubes using this technique.

3.1. Mechanical and electronic properties of carbon nanotubes

HRTEM studies reveal that CNTs are extraordinarily flexible and do not break upon mechanical deformation. For example, they can be bent mechanically by mechanical milling, or by

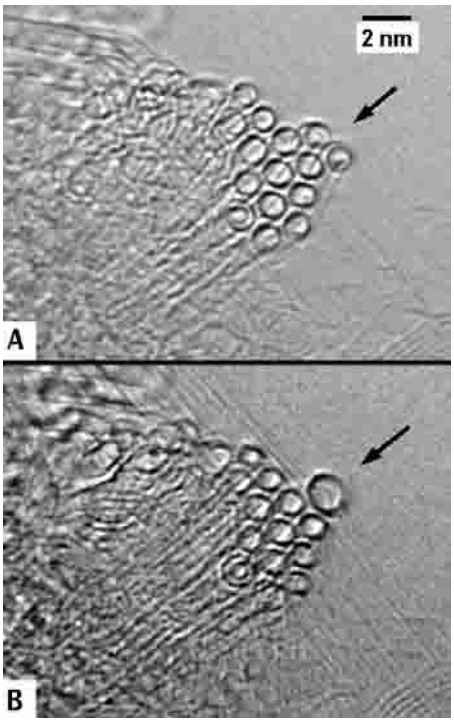

Figure 14. Coalescence of single-walled CNTs. (A) Before coalescence. (B) After coalescence.

embedding the tubes in a polymeric resin [58], [66]–[68]. Theoretical calculations predict this flexibility [69]–[71]. The first attempt to determine the stiffness of CNTs was carried out by Treacy and colleagues. Using a HRTEM to measure the amplitudes of vibrating tubes at different temperatures, the authors calculated indirectly Young's modulus [45, 72]. They found that MWCNTs exhibit Young's moduli of the order of 1.8 TPa, which is higher than conventional carbon fibres (about 800 GPa). Direct measurements using atomic force microscopy (AFM) revealed that the Young's modulus of MWCNTs is around 1.28 TPa [72, 73]. This high Young's modulus makes CNTs a very strong material. However, the challenge of building a super-strong composite material out of nanotubes is still underway.

The first measurements of the electrical conductivity of MWCNTs were recorded using gold micro-contacts attached to the tubes by lithographic techniques. These showed that the resistance depends on the temperature and that in the range between 2 and 300 K the tubes were semimetallic [73]. Conductivity measurements on aligned MWCNTs show that the material behaves as a nanoconductor [74, 75]. For SWCNTs, it was confirmed that, depending on the diameter and chirality, CNTs could be metallic conductors or semiconductors [76, 77]. SWCNTs around 14 Å in diameter also exhibit quantum (discrete) electronic conductivity [76]. It is noteworthy that the atomic arrangement (the geometry of the structure) determines the mechanical and electronic properties of CNTs. Nowadays, the production of CNT crystals has been reported [78]. Unfortunately, these experiments have not been reproduced by other groups.

It has been observed (*in situ*) that SWCNTs can coalesce under high electron irradiation and high temperature conditions (around 800 °C, figure 14) [79]. Tight binding molecular dynamic (TBMD) calculations suggest that vacancies, generated by knock-on displacements of carbon

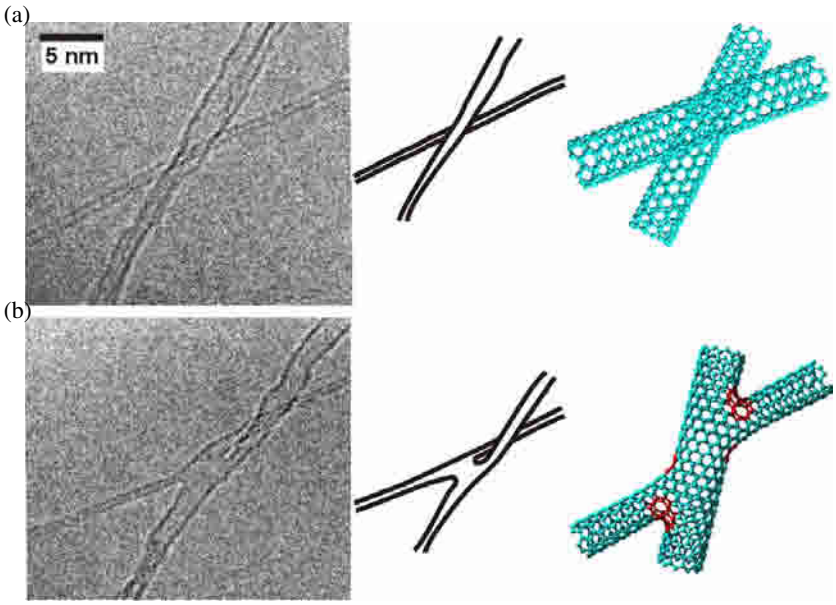

Figure 15. Nanotube junctions under the electron beam: (a) two tubes before connection; (b) nanotube junction after connection.

atoms by fast electrons inside the electron microscope, trigger this coalescence [79]. Moreover, in order to achieve coalescence, the tubes should possess the same chirality, otherwise tube polymerization might take place. Recent experiments by Terrones and colleagues [80] have shown that CNT junctions can be produced under similar conditions (see figure 15); this opens up the possibility of synthesizing CNT networks and novel resistant and lightweight carbon fabrics.

4. Boron nitride nanotubes

hBN is another layered material with a structure very similar to graphite, having hBN ring layers separated by 3.33 Å, in which every boron is connected to three nitrogen atoms and vice versa; the B–N distance is 1.44 Å. Between the layers, every boron interacts with a nitrogen atom through a van der Waals force (figure 16). Bulk hBN is an insulator with a bandgap of 5.8 eV [81], whereas graphite is a semimetal (band overlap = 0.04 eV) [57]. The first groups who reported the existence of BN nanotubes used the electric arc discharge method with high melting point metal (tantalum and tungsten, for example) electrodes and BN powder inside the anode [82]–[84]. Loiseau *et al* [85] reported the production of BN nanotubes by arcing HfB_2 electrodes in an inert atmosphere. This technique led to the formation of mainly single- and double-walled BN tubes.

It was noticed that, in BN nanotubes, the tips were squared, meaning that instead of having pentagonal rings to close the structure (as in CNTs), there are BN squares. This is energetically more favorable because a pentagon will exhibit B–B or N–N bonds, which are more unstable. In terms of curvature, BN admits, with high stability, squares for the positive curvature and octagons for the negative curvature. Nevertheless, Fowler and colleagues have found using density functional tight binding (DFTB) calculations that nitrogen excess in BN cages is stable [86].

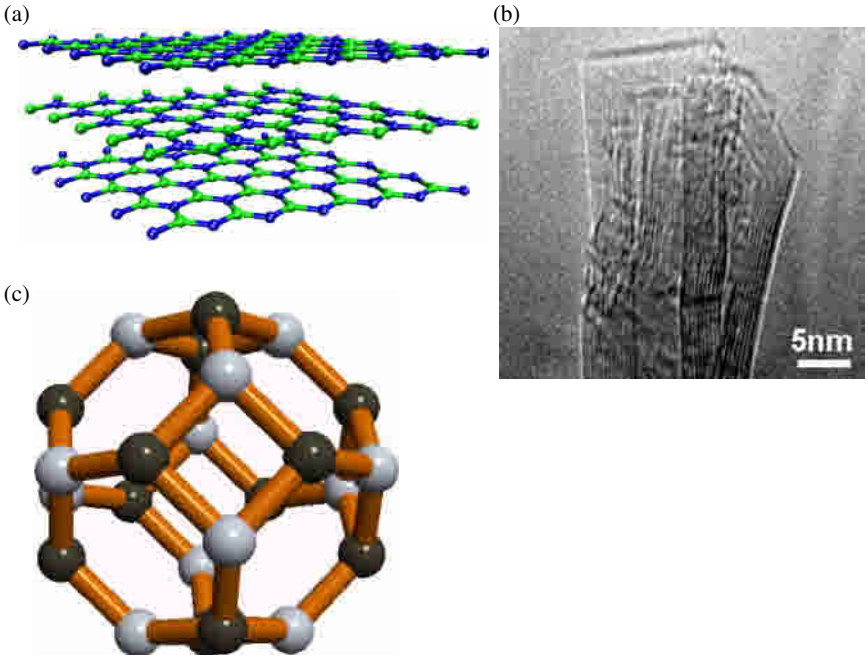

Figure 16. (a) Boron nitride layered structure. (b) Boron nitride nanotubes synthesized with the electric arc discharge method. (c) Fullerene made of boron nitride by the introduction of squares.

Theoretical studies revealed that BN nanotubes are insulators with a bandgap of 5.5 eV [87], a bit smaller than in bulk BN. This property is independent of tube diameter, chirality and number of walls. BN nanotubes may also be extremely resistant to oxidation and have exhibited high Young's moduli (see below). Therefore, the tubes may find important uses in ceramics and composites.

Han *et al* [88] reported the efficient generation of BN nanotubes by reacting pyrolytically grown CNTs with B_2O_3 in the presence of N_2 at high temperatures (1300–1500 °C). Subsequent studies by Golberg *et al* [89] have shown that BN nanotube bundles can also be produced in bundles when CNTs are exposed to mixtures of B_2O_3, V_2O_5 and MoO_3 in a N_2 atmosphere at elevated temperatures. Very recently, alternative experimental approaches have been developed in order to generate BN nanotubes and other BN nanostructures:

(a) thermolysis of borazine ($B_3N_3H_6$) over nickel boride catalyst particles at 1000–1100 °C [90];
(b) thermal annealing of powdered rhombohedral boron and hBN mixtures at 1200 °C in lithium vapour [91];
(c) plasma jets [92, 93], and
(d) ball milling of hBN, followed by thermal annealing at 1300 °C [94, 95].

At this stage, novel composites and nanoscale components need to be fabricated employing BN nanotubes, which appear to be extremely resistant to oxidation. Experimental determination of the Young's modulus of BN tubes ($Y = 1.22 \pm 0.24$ TPa) [96] confirms the values obtained using theoretical approaches for BN nanotubes [97, 98] and reveals that BN tubes are highly crystalline and may be the strongest insulating nanofibres.

(a)

(b)

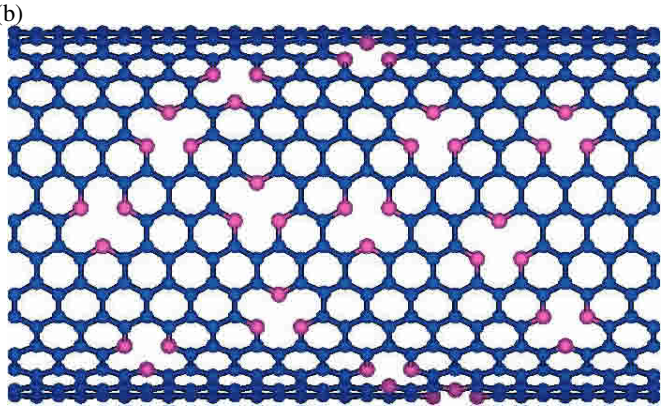

Figure 17. Nitrogen-doped carbon nanofibres. (a) TEM micrograph of aligned nitrogen-doped nanofibres. (b) Computer model of a nitrogen-doped nanotube showing the nitrogen islands (nitrogen is just coordinated to two carbons: pyridine-like bonding).

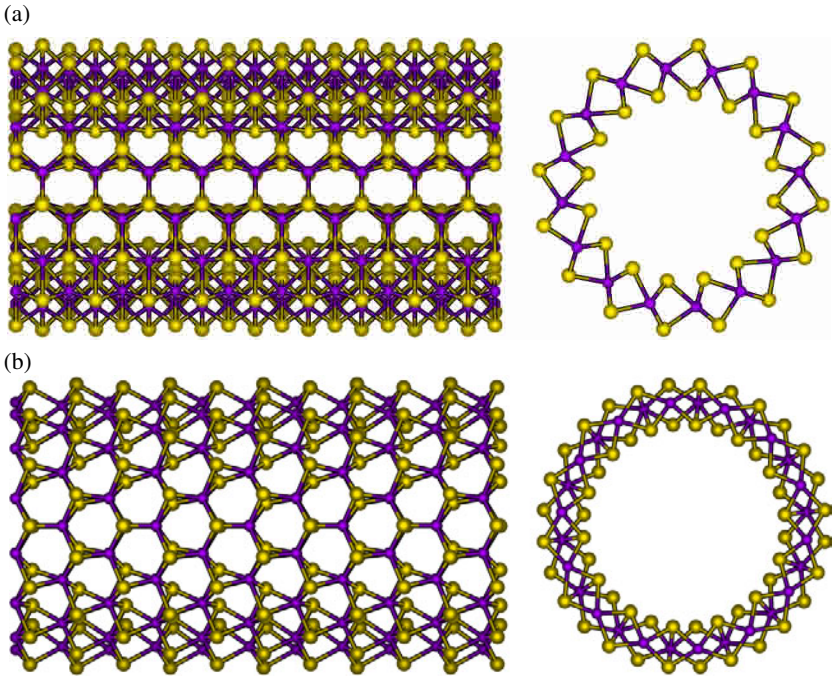

Figure 18. Molybdenum disulfide nanotubes. (a) Armchair type nanotube. (b) Zig-zag type nanotube (light atoms are sulfur, dark atoms are molybdenum).

Graphite and hBN have opened new possibilities for producing novel nanomaterials with different types of $B_xC_yN_z$ systems [99]. Pyrolysis experiments with melamine (trisaminotriazine) have been helpful in synthesizing C_xN_y nanofibres: Terrones *et al* [100, 101] described nanotubes with stoichiometries close to $C_{12}N$ and confirmed that nitrogen is bonded in a sp^2 fashion within the carbon framework.

Boron-doped CNTs have also been synthesized by electric arc discharge with hBN inside the graphite anode [102]. In this experiment it is noticed that CNTs are highly graphitic and also very long, around 20–100 μm. It was found that B was usually located at the tips of the tubes and that the zig-zag chirality was preferred among tubes [102]. Blase and colleagues found using molecular dynamics *ab initio* calculations that boron was acting as a surfactant, avoiding the zig-zag tubes closure [102]. In addition, boron-doped CNTs exhibit conducting properties.

On the other hand, nitrogen-doped CNTs can also exhibit fascinating features such as pyridine-like species within the graphitic mesh (figure 17) [103], which causes a peak close to the Fermi level in the local density of states (LDOS). All these nanotubes, armchair and zig-zag are found to be metallic. Therefore, the nitrogen is donating electrons to the nanotube system in order to enhance electronic transport.

5. Metal dichalcogenide curved nanostructures

Another type of layered material that can be bent are molybdenum and tungsten disulfides (MoS_2 and WS_2). The most stable forms of MoS_2 and WS_2 consist of a metal layer sandwiched between two sulfur layers (space group $P63/mmc$). These triple layers are stacked together, similar to graphite, by van der Waals interactions separated by 6.15 Å for MoS_2 and 6.18 Å for WS_2. In 1992

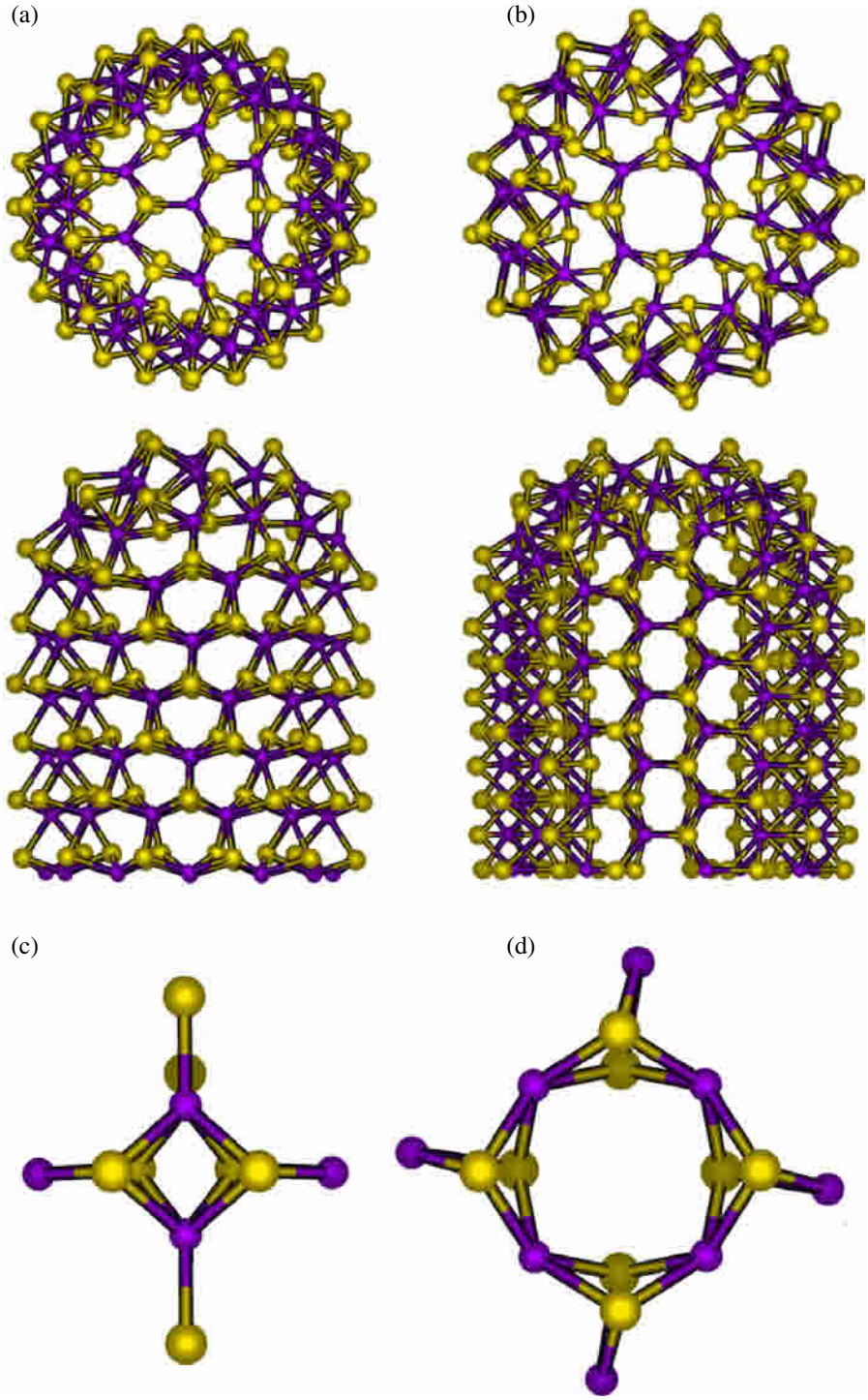

Figure 19. Nanotube caps of molybdenum disulfide nanotubes. (a) Closing a zig-zag nanotube with 3 SLD. (b) Closing an armchair nanotube with 4 SLD and 1 OLD; (c) SLD; (d) OLD.

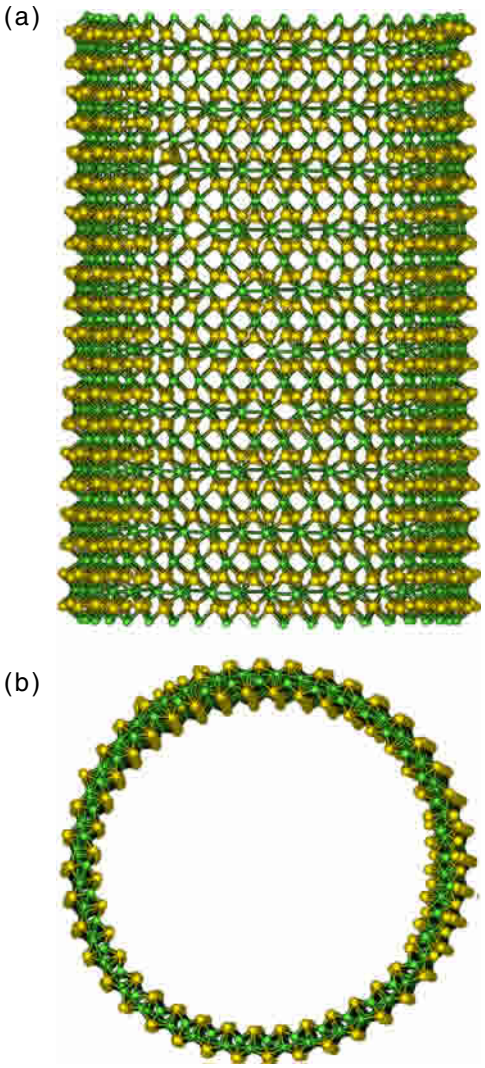

Figure 20. Rhenium sulfide nanotube: (a) side view; (b) top view.

Reshef Tenne's group found that MoS_2 and WS_2 could form closed cages (inorganic analogues of fullerenes) and nanotubes by substitution reactions under H_2S atmospheres [104]–[106]. These nanostructures have proved to be exceptional solid lubricants [107].

DFTB calculations demonstrated that both armchair and zig-zag MoS_2 and WS_2 are semiconductors, with a gap decreasing as the diameter decreases. In bulk, flat MoS_2 and WS_2 layers exhibit a semiconducting behaviour with a larger gap than that observed for the respective nanotubes [108, 109]. Interestingly, armchair nanotubes exhibit indirect and direct gaps, similar to the bulk material, whereas zig-zag tubes only display direct gaps. Nevertheless, all MoS_2 and WS_2 nanotubes will be semiconducting (figure 18).

In order to close MoS_2 and WS_2 layers, preserving the stoichiometry, square-like defects (SLD) and octagonal-like defects (OLD) are needed. In figure 19 we show how to achieve closure in zig-zag and armchair disulfide nanotubes. Note that the positive curvature is given by the SLD and the negative curvature by the OLD. Inorganic fullerenes will need 6 SLD to close the cage [109] (figure 19).

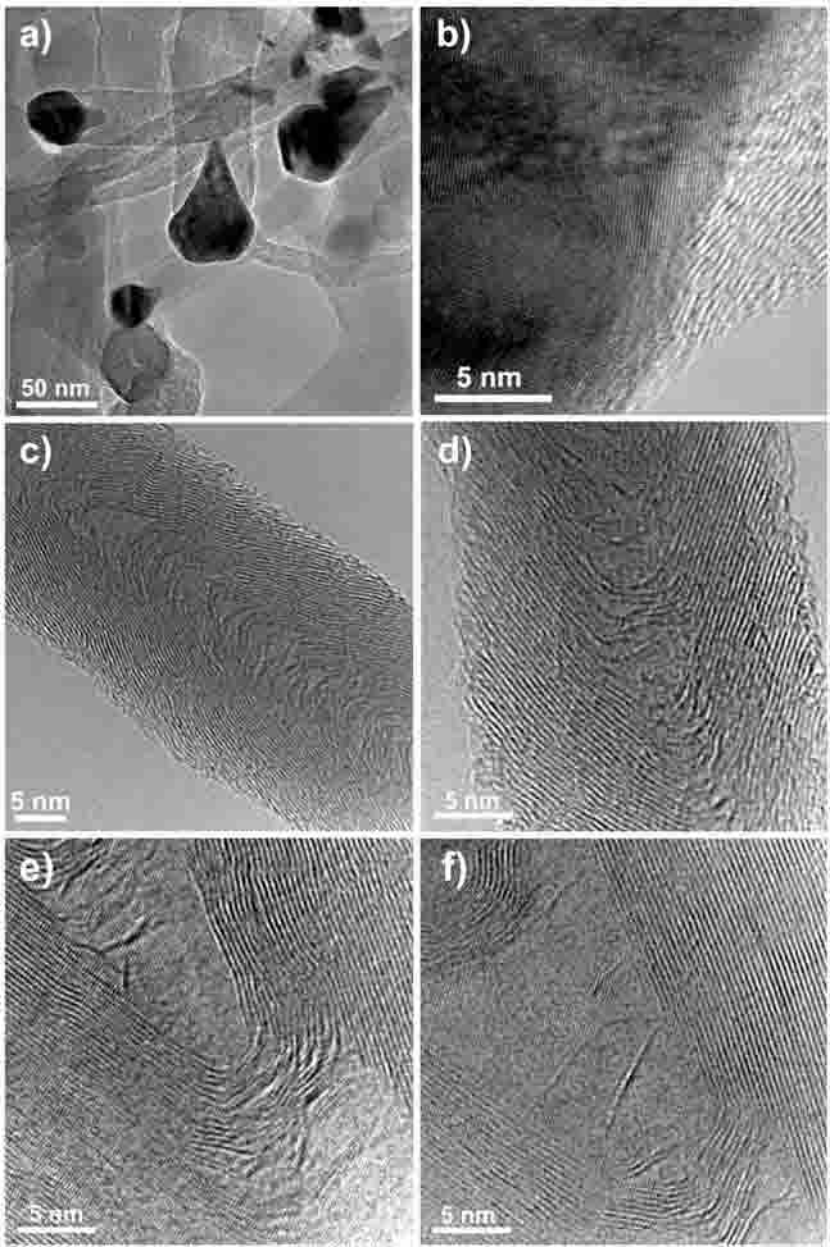

Figure 21. Carbon nanocones. (a) Transmission electron micrograph of nanocone fibres showing the palladium conical particle at the tip. (b) High resolution electron micrograph (HRTEM) of the palladium–carbon interface. Note the graphitic and palladium lattice. (c)–(f) HRTEM of different nanofibres formed by stacking carbon nanocones.

Rao's group [110] reported the existence of NbS_2 and TaS_2 nanotubes by hydrogen reduction of trisulfides NbS_3 and TaS_3 at 700 °C; in this work, there are also nanoribbons. DFTB calculations on NbS_2 nanotubes reveal that all of them are metallic [111]. The metallic character of these tubes arises from the fact that Nb has one d electron less than Mo or W in the valence shell. In fact, the flat layer of NbS_2 is metallic and becomes a superconductor around 6–7 K.

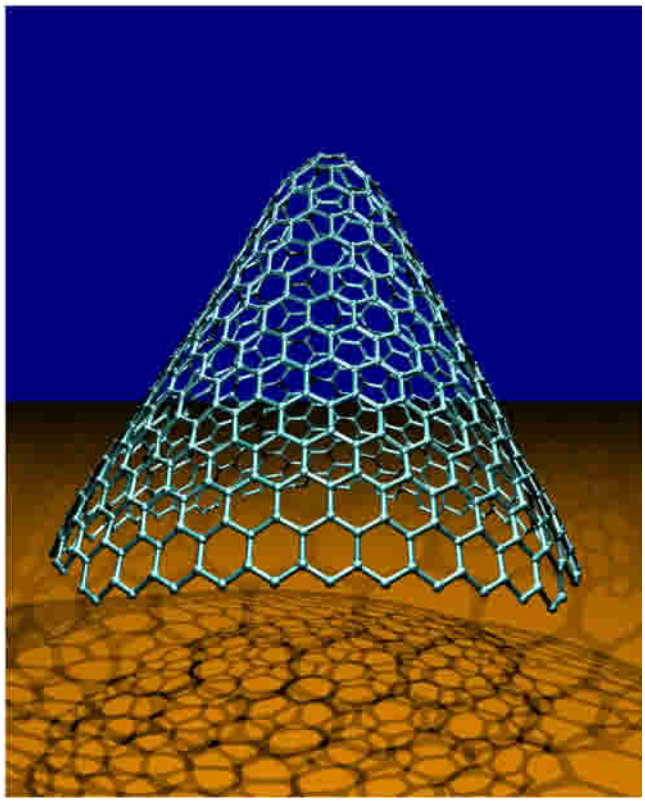

Figure 22. Computer model of a carbon nanocone.

Table 1. The three smallest cases of Schwarzites. Name, space group, lattice parameter, number of atoms in the cubic cell and fractional coordinates are given. The genus per primitive cell in each case is 3.

Name	SPGR	Lattice constant (Å)	N atom	x	y	z
D688	$Pn\bar{3}m$ (224)	6.148	24	0.5	0.333 42	0.666 58
P688	$Im\bar{3}m$ (229)	7.828	48	0.319 52	0.319 52	0.093 73
G688	$Ia\bar{3}d$ (230)	9.620	96	0.922 05	0.120 94	0.955 02

Table 2. Schwarzite P8bal, space group, lattice parameter, number of atoms in the cubic cell and fractional coordinates are given. The genus per primitive cell is 3. This structure divides space into two equal regions.

Name	SPGR	Lattice constant (Å)	N atom	x	y	z
P8bal	$Im\bar{3}m$ (229)	15.043	192	0.324 62	0.090 57	0.32 462
				0.289 45	0.172 26	0.289 45
				0.399 48	0.048 20	0.280 96

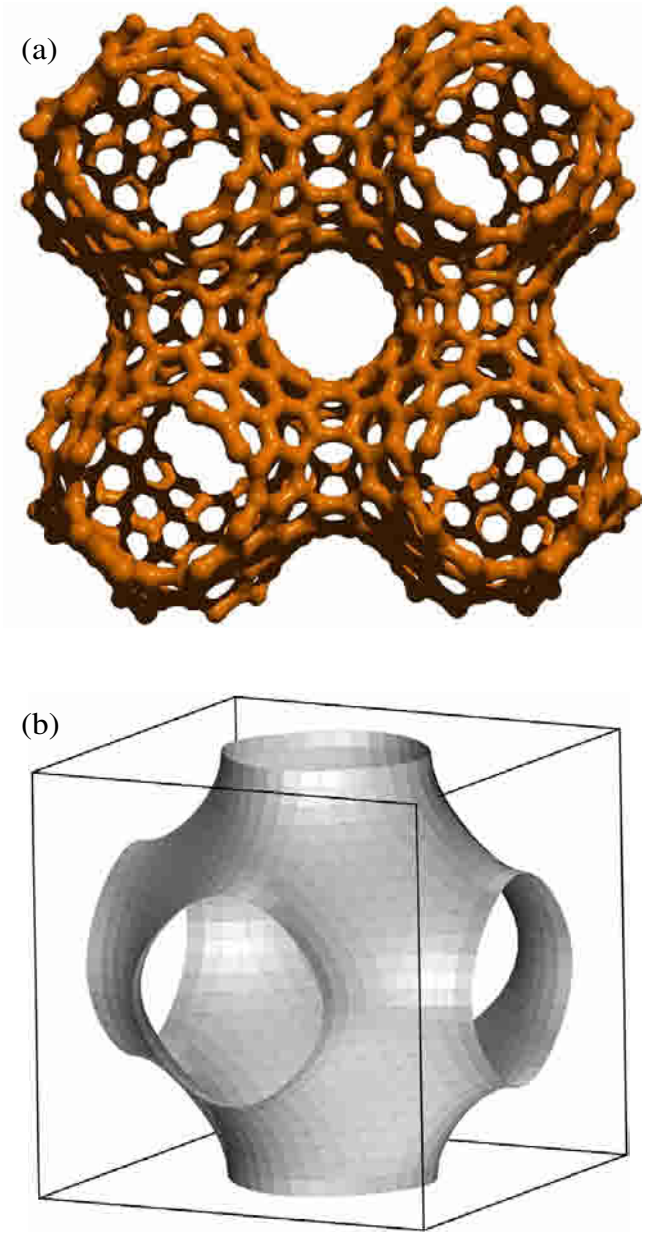

Figure 23. (a) Four cubic cells of the P (primitive) TPMS decorated with graphite using hexagonal and octagonal rings of carbon (192 atoms per cubic cell). (b) The P TPMS.

Recently, ReS_2 nanocages and nanotubes have been synthesized by direct sulfidization of ReO_2 formed from the decomposition of ReO_3 under the flow of nitrogen at 700 °C (figure 20) [112, 113].

5.1. Nanowires

Fullerenes and CNTs are hollow, so it should be possible to fill them up with different elements or compounds. Introducing a metal inside a CNT might form a nanowire. Using an electric

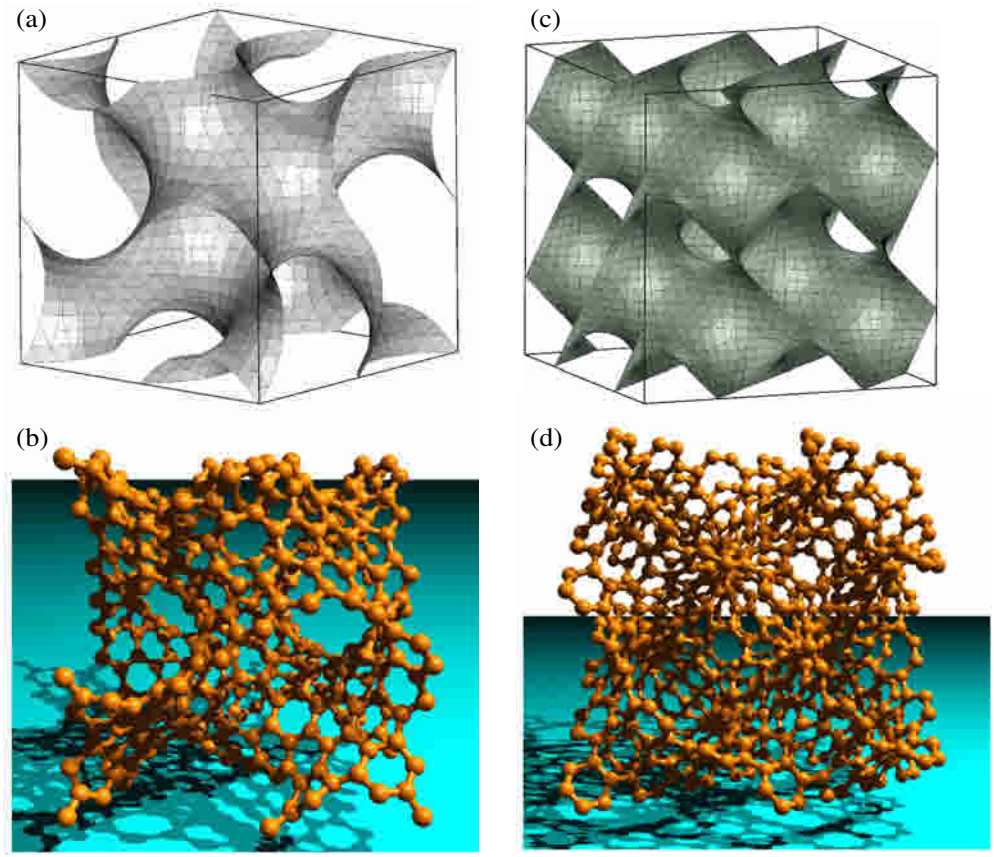

Figure 24. (a) The *G* (gyroid) TPMS. (b) One cubic cell of the *G* TPMS decorated with graphite using hexagonal and octagonal rings of carbon (384 atoms per cubic cell). (c) The *D* (diamond) TPMS. (d) One cubic cell of the *D* TPMS decorated with graphite using hexagonal and octagonal rings of carbon (768 atoms per cubic cell).

arc discharge with a metal powder inside the anode, one could produce CNTs filled with metal carbides [68], [114]–[116]. A difficulty with the method mentioned above is that the tubes are only partly filled; this might affect the conductivity properties. Loisseau and Pascard [117] found that nanotubes could be filled significantly when small amounts of sulfur are involved in the electric arc experiments. Moreover, there are chemical techniques (using nitric acid treatments), in which the tubes can be opened and nanomaterials, such as oxides of Pd, Ag, Au, Co, Fe, Ur, Ni, Mo, Sn, Ny, Eu, La, Ce, Y, Zr and Cd, could be inserted into their interior [118]–[122]. It is also important to mention that enzymes and proteins have been introduced inside nanotubes [123, 124]. On the other hand, capillarity effects have been used to introduce elements inside CNTs such as Sn, Pb, Bi, Cs, S and Se [125]–[127].

Pyrolysis experiments with ferrocene ($FeCp_2$) and C_{60} have proved to be very useful to produce aligned Fe-filled carbon MWCNTs [128]. Magnetic measurements on these tubes indicate that they possess higher magnetic coercivities than those reported for nickel and cobalt nanowires [128]. It is noteworthy that the graphene layers avoid oxidation, protecting very well these ferromagnetic nanowires. It is believed that Fe nanowires might find applications as magnetic storage devices. Recently, it has been found that spray pyrolysis of mixtures of

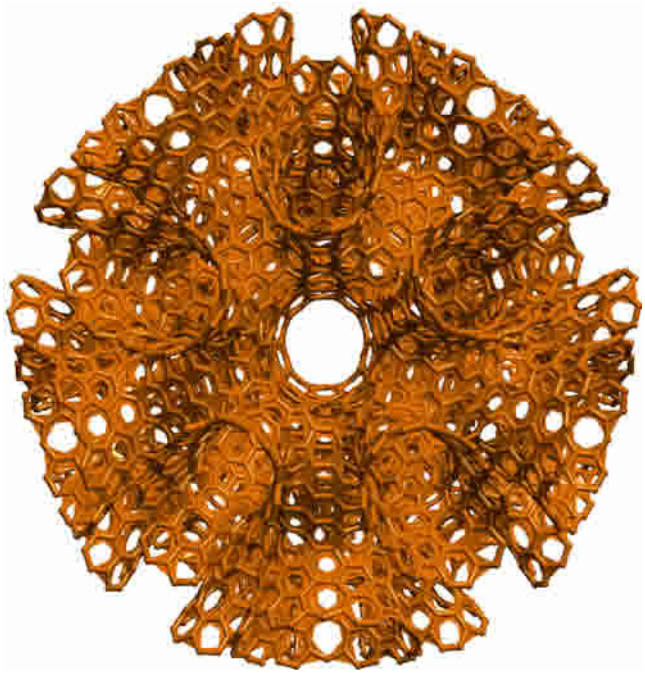

Figure 25. Quasi-periodic graphitic structure with I_h symmetry oriented along the five-fold axis.

Table 3. Schwarzite G8bal name, space group, lattice parameter, number of atoms in the cubic cell and fractional coordinates are given. The genus per primitive cell is 3. This structure divides space into two equal regions.

Name	SPGR	Lattice constant (Å)	N atom	x	y	z
G8bal	$Ia\bar{3}d$ (230)	18.599	384	0.188 12	0.209 68	0.770 90
				0.128 05	0.168 39	0.794 76
				0.076 32	0.201 51	0.843 64
				0.020 66	0.155 94	0.873 48

Table 4. Schwarzite D8bal, space group, lattice parameter, number of atoms in the cubic cell and fractional coordinates are given. The genus per primitive cell is 3. This structure divides space into two equal regions.

Name	SPGR	Lattice constant (Å)	N atom	x	y	z
D8bal	$Fd\bar{3}m$ (227)	23.731	768	0.042 30	0.000 00	0.457 70
				0.084 55	0.000 00	0.415 45
				0.097 91	0.054 08	0.389 13
				0.152 09	0.054 08	0.360 87
				0.207 70	0.000 00	0.292 30
				0.165 45	0.000 00	0.334 55

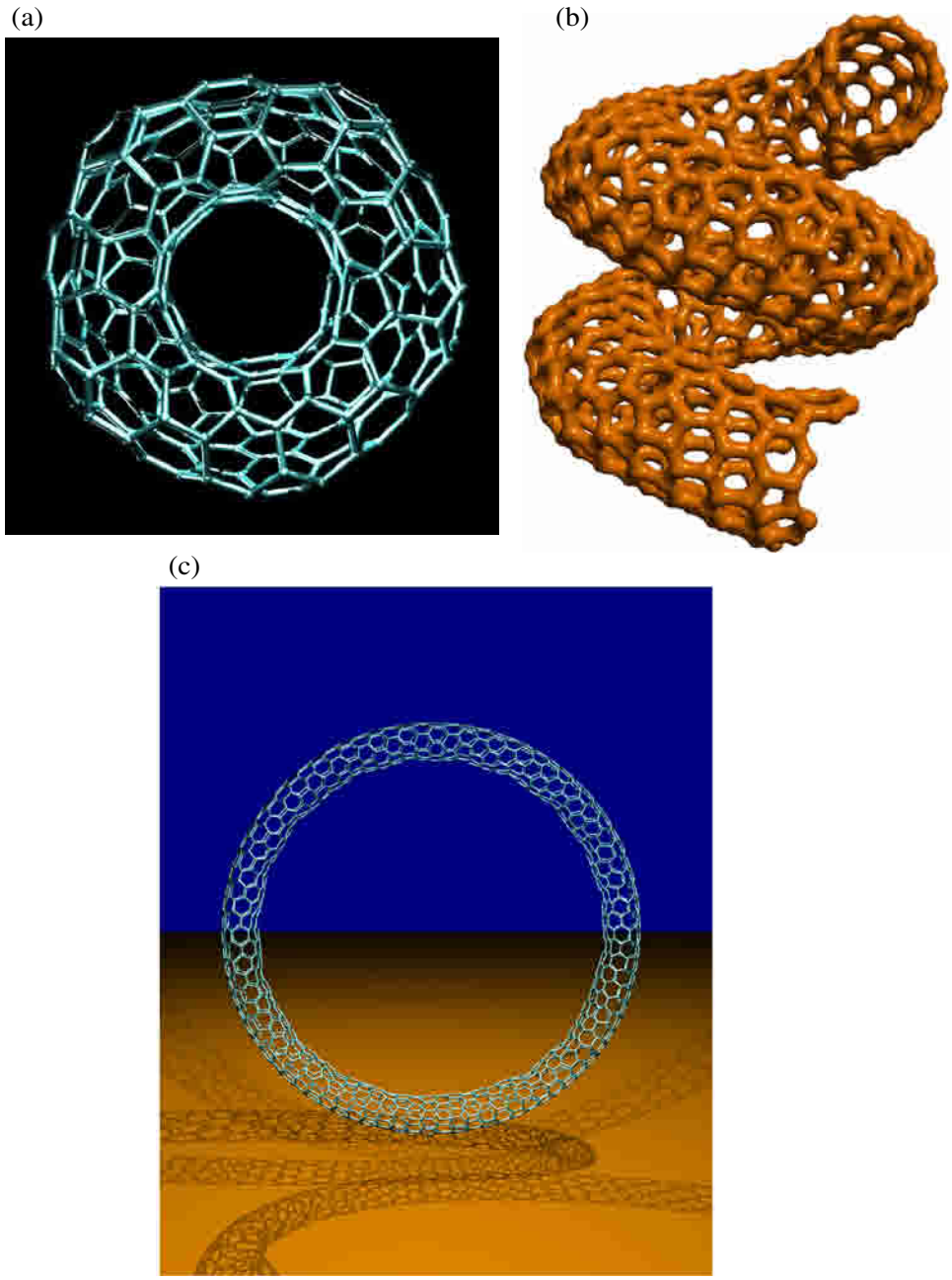

Figure 26. (a) Torus decorated with graphite with heptagons, pentagons and hexagons. (b) Helicoidal graphite with heptagons, pentagons and hexagons. (c) Torus decorated with graphite formed by joining the opposite ends of a (8, 0) nanotube, possessing just hexagons.

nickelocene ($NiCp_2$) and ferrocene in benzene produce nanowires with a Ni–Fe alloy called invar ($Fe_{65}Ni_{35}$) [129]. In the future, we expect that pyrolysis techniques will enable more control of the filling of the nanotube in order to produce nanowires with exact alloy compositions.

An alternative to filling MWCNTs is by electrolysis of graphite electrodes in molten salts containing small amounts of tin, bismuth or lead chloride [130].

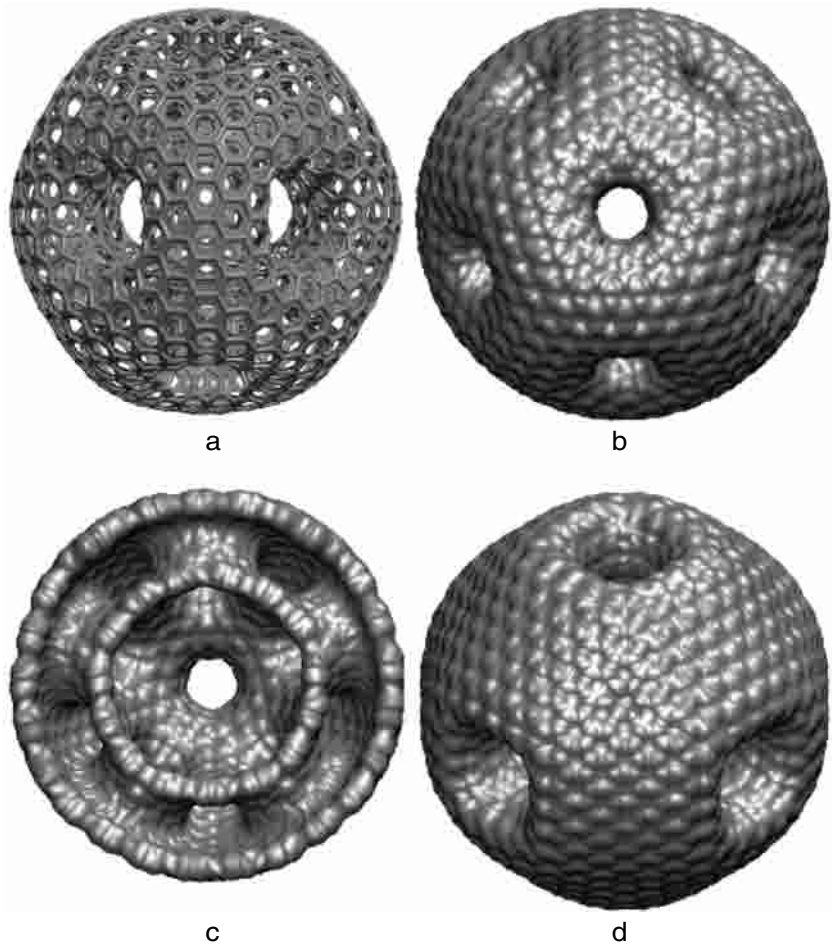

Figure 27. High genus fullerenes with heptagons and hexagons (no pentagons) holey balls. (a) Two-fold axis of a 2040-atom genus 11 fullerene. (b) Five-fold axis. (c) Cut perpendicular to the five-fold axis. (d) A genus 5 holey ball with 1896 atoms.

Table 5. Schwarzite D766, space group, lattice parameter, number of atoms in the cubic cell and fractional coordinates are given. The genus per primitive cell is 3. This structure divides space into two different regions.

Name	SPGR	Lattice constant (Å)	N atom	x	y	z
D766	$Fd\bar{3}$ (203)	23.206	672	0.113 35	0.002 82	0.244 80
				0.991 21	0.031 76	0.213 73
				0.023 67	0.072 66	0.254 65
				0.908 03	0.076 47	0.160 39
				0.930 92	0.140 53	0.156 54
				0.926 14	0.042 53	0.215 12
				0.815 33	0.009 36	0.159 54

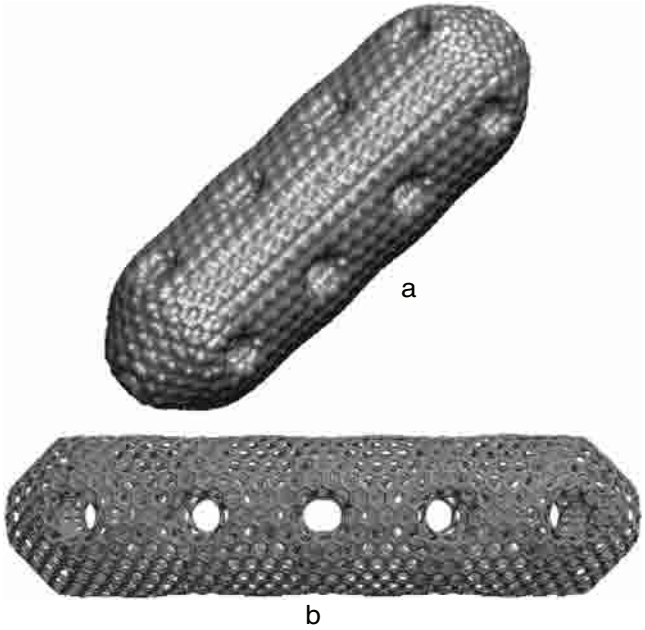

Figure 28. Holey tubes with heptagons and hexagons (no pentagons). (a) Genus 17 holey tube with 2880 atoms. (b) Genus 21 holey tube with 3568 atoms.

Table 6. Schwarzite P7par, space group, lattice parameter, number of atoms in the cubic cell and fractional coordinates are given. The genus per primitive cell is 3. This structure divides space into two different regions.

Name	SPGR	Lattice constant (Å)	N atom	x	y	z
P7par	$Pm\bar{3}m$ (221)	16.394	216	0.274 60	0.148 50	0.211 41
				0.455 50	0.140 91	0.140 91
				0.411 25	0.075 85	0.179 23
				0.327 51	0.077 05	0.206 09
				0.455 99	0.000 00	0.181 51
				0.295 29	0.000 00	0.234 26

It is important to note that other types of inorganic materials, fullerenes and gases have also been incorporated inside the cylindrical cores of SWCNTs and MWCNTs. However, this topic is beyond the scope of this review.

6. Carbon nanocones

Theoretical studies predicted the formation of graphitic cones [131, 132]. Subsequently, isolated graphitic cones were produced by carbon condensation on a graphite substrate [133] and by pyrolysis of heavy oils [134]. More recently, single-walled aggregates of conical graphitic

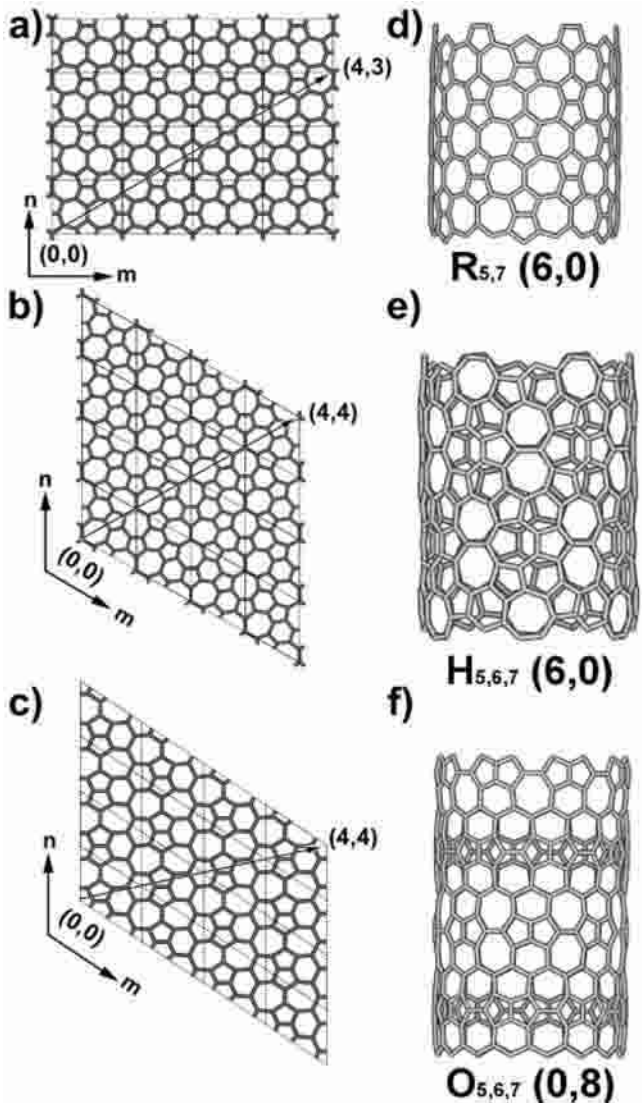

Figure 29. Haeckelites. (a) Rectangular Haeckelite sheet (R). (b) Hexagonal Haeckelite sheet (H). (c) Oblique Haeckelite sheet (O). (d)–(f) are the corresponding Haeckelite tubes. All Haeckelites are metallic sheets and tubes.

structures have been prepared by laser ablation of graphite targets [135]. Conical structures consisting of other layered materials such as BN have also been prepared by reacting boron oxide vapours with MWCNTs [136].

Very recently, it was found that pyrolysis of palladium precursors always produces conical nanofibres (figure 21) [137]. An important feature of these new nanostructures is that they are held together by van der Waals forces since the fibre is composed of an arrangement of stacked cones, which could be opened or closed (figure 22). It is believed that nanocones may be good electron field emitters. Charlier's group has calculated the electronic properties of nanocones, finding that there is a charge accumulation towards the tip and that these are localized states near the Fermi level (E_F). These features make them suitable as field emitters [138].

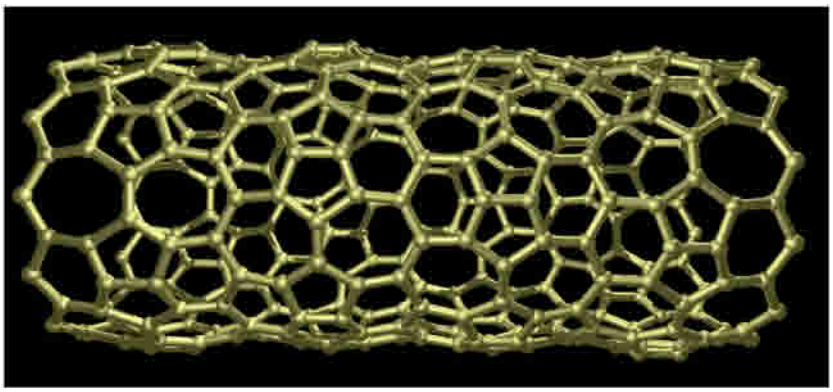

Figure 30. Corrugated Haeckelite oblique tube.

Table 7. Schwarzite IWPg, space group, lattice parameter, number of atoms in the cubic cell and fractional coordinates are given. The genus per primitive cell is 4. This structure divides space into two different regions.

Name	SPGR	Lattice constant (Å)	N atom	x	y	z
IWPg	$I\bar{4}3m$ (217)	24.349	744	0.074 76	0.006 41	0.379 90
				0.101 51	0.058 91	0.374 25
				0.158 56	0.058 09	0.358 62
				0.248 07	0.207 00	0.453 54
				0.200 22	0.157 47	0.383 10
				0.200 38	0.102 52	0.360 05
				0.178 46	0.002 32	0.344 60
				0.225 27	0.001 93	0.309 53
				0.253 03	0.170 55	0.409 86
				0.019 75	0.019 75	0.385 66
				0.092 08	0.253 80	0.335 54
				0.048 76	0.257 29	0.298 34
				0.050 63	0.094 49	0.626 79
				0.052 09	0.152 71	0.643 56
				0.151 22	0.193 56	0.618 61
				0.097 63	0.193 78	0.643 86

Table 8. Hexagonal Haeckelite crystal made of pentagons, hexagons and heptagons. Name, space group, lattice constants and fractional coordinates are given. The distance between layers has been set at 3.42 Å.

Name	SPGR	Lattice constants (Å)	x	y	z
H567	$p321$ (150)	$a = b = 7.083$, $c = 3.42$	0.000 00	0.000 00	0.000 00
			0.179 93	0.431 92	0.000 00
			0.111 52	0.590 28	0.000 00
			0.000 00	0.209 62	0.000 00

Table 9. Oblique Haeckelite crystal made of pentagons, hexagons and heptagons. Name, space group, lattice constants and fractional coordinates are given. The distance between layers has been set at 3.42 Å.

Name	SPGR	Lattice constants (Å)	x	y	z
0567	$p1$ (1)	$a = 7.224$, $b = 5.453$, $c = 3.42$	0.206 26	0.156 06	0.000 00
		$\alpha = \beta = 90°$, $\gamma = 124.319°$	0.112 63	0.315 12	0.000 00
			0.118 31	0.860 10	0.000 00
			0.523 64	0.163 46	0.000 00
			0.430 01	0.322 52	0.000 00
			0.517 97	0.618 48	0.000 00
			0.870 47	0.153 97	0.000 00
			0.765 80	0.324 61	0.000 00
			0.878 46	0.658 86	0.000 00
			0.757 81	0.819 72	0.000 00
			0.320 44	0.866 82	0.000 00
			0.315 83	0.611 75	0.000 00

Table 10. Rectangular Haeckelite crystal made of pentagons, hexagons and heptagons. Name, space group, lattice constants and fractional coordinates are given. The distance between layers has been set at 3.42 Å.

Name	SPGR	Lattice constants (Å)	x	y	z
R57	$C2$ (5)	$a = 7.454$, $b = 5.831$, $c = 3.42$	0.000 00	0.001 81	0.000 00
		$\alpha = \beta = \gamma = 90°$	0.156 34	0.151 33	0.000 00
			0.500 00	0.252 02	0.000 00
			0.091 47	0.376 91	0.000 00
			0.343 66	0.102 49	0.000 00

7. Negatively curved graphite 'Schwarzites'

In 1991, Mackay and Terrones [13] proposed that the inclusion of carbon rings with more than six atoms in a graphite hexagonal mesh could produce stable periodic graphitic arrangements with negative curvature analogous to zeolites (figure 23). These new hypothetical arrangements, called 'Schwarzites', exhibit topologies similar to the TPMS [9, 10], [13]–[15], which have attracted mathematicians since the 1890s (see figure 24). TPMS possess, at all their points, zero mean curvature, so $H = 0$ everywhere. Schwarzites and TPMS show labyrinths that can divide space into two congruent regions. Energetic calculations have been performed in Schwarzites; they are more stable than C_{60} [139]–[142]. This stability comes from the fact that in the heptagonal or octagonal rings there is very little mechanical strain, thus preserving the sp^2-*like* nature of graphite (120° angles between nearest neighbours). As we have observed earlier, the heptagons or octagons generate negative curvature or saddle points necessary for periodicity and complexity. The genus per primitive cell of the most common Schwarzites is 3 and 4 [143], so they are more complex than fullerenes, which possess genus 0 (see equation (1)).

Among the possible applications of Schwarzites we can suggest: semiconducting nanodevices, new catalysts and molecular sieves. Heptagonal rings of carbon not only produce periodicity, but also can generate quasi-periodicity or disorder in a graphitic architecture [144] (see figure 25). Fractional coordinates and characteristic features of Schwarzites are given in tables 1–7.

We have seen that complexity and periodicity are linked with the number of rings (higher than six carbon atoms; see equation (1)). One question emerges here: can we propose a closed complex structure (genus greater than zero) without periodicity? The answer is yes. Itoh, Ihara and Kitakami have shown that toroidal graphite is stable. These tori exhibit genus 1 ($g = 1$) possessing pentagons, hexagons and heptagons [145, 146] (see figure 26). Also, helicoidal graphitic tubes have been found experimentally [147]. However, the most complex hypothetical arrangements have been proposed by Terrones and Terrones [144]. These structures lack pentagonal rings and contain only heptagons and hexagons. The genus of these structures goes up to $g = 21$, having the same topology as a sphere with 21 handles (figures 27 and 28). An important feature of the complex graphitic structures is that they exhibit holes or labyrinths, in which molecules can be inserted. TB calculations showed that around the holes (necks), the electronic behaviour is metallic [148].

7.1. Haeckelites

The presence of defects such as pentagons and heptagons in fullerenes modifies the electronic properties. A new hypothetical type of graphene sheet, which admits pentagons, heptagons and hexagons, has been proposed, noting that the number of heptagons and pentagons should be the same in order to compensate for the negative curvature of the heptagons and the positive curvature of the pentagons [149] (figure 29). These arrangements are now called 'Haeckelites' in honour of Ernst Haeckel, a German zoologist who produced a beautiful drawing of radiolaria (micro-skeleta of zoo-plankton), in which heptagonal, hexagonal and pentagonal rings were observed [150]. An important property of Haeckelites is that they all exhibit a significant electronic signal at E_F in the LDOS. This means that all these systems should possess metallic behaviour. Thus, it is possible to roll up Haeckelite sheets to form nanotubes, which will be conductors, independent of the diameter and chirality.

Another property of Haeckelite tubes is that they keep the stiffness of classical CNTs, composed of only hexagons; the Young's modulus of Haeckelite tubes is around 1.0 TPa. In addition, Haeckelites also exhibit local rugosity due to the local curvature introduced by the presence of heptagons and pentagons (figure 30). It might be possible that electron irradiation experiments generate heptagon–pentagon pairs (rugosity) in SWCNTs. For fractional coordinates of Haeckelites see tables 8–10.

8. Conclusions

Different layered materials could curve and bend in order to form various nanostructures with novel properties. Graphite is just one example of a planar structure that can be transformed into fullerenes, nanotubes (multi-walled or single-walled), nanocones, etc. However, hBN, WS_2, MoS_2, NbS_2 and ReS_2 could also be bent in order to form new nanostructures. Computer simulations and experimental work indicate that curvature, introduced via different types of 'defects', produces stable atomic arrangements. These 'defects', which can be pentagons, heptagons, rings with more atoms, or even more complex architectures, modify the electronic,

magnetic and mechanical properties of the systems. Along this line, doping of curved nanostructures is a promising area of research. We are at the beginning of a new field in which new curved layered nanomaterials are waiting to be discovered. At present the main challenge is to control their production and to generate larger amounts with specific characteristics so that the fabrication of novel nanotechnological devices becomes a reality in the twenty-first century.

Acknowledgments

Support from CONACyT-México, through grants W-8001, 36365-E and G-25851-E and 37589-U is gratefully acknowledged.

References

[1] Kroto H W, Heath J R, Obrien S C, Curl R F and Smalley R E 1985 *Nature* **318** 162
[2] Krätschmer W, Lamb L D, Fostiropoulos K and Huffman D R 1990 *Nature* **347** 354
[3] Iijima S 1991 *Nature* **354** 56
[4] Bockrath M, Cobden D H, McEuen P L, Chopra N G, Zettl A and Smalley R E 1997 *Science* **275** 1922
[5] Tans S J, Verschueren A R M and Dekker C 1998 *Nature* **393** 49
[6] Kwon Y-K, Tománek D and Iijima S 1999 *Phys. Rev. Lett.* **82** 1470
[7] Ebbesen T W 1996 *Phys. Today* **49** 26
[8] Yakobson B I and Smalley R E 1997 *Am. Sci.* **83** 324
[9] Terrones H and Mackay A L 1992 *Carbon* **30** 1251
[10] Mackay A L and Terrones H 1993 *Phil. Trans. R. Soc.* A **343** 113
[11] Ugarte D 1992 *Nature* **359** 707
[12] Ugarte D 1993 *Chem. Phys. Lett.* **207** 473
[13] Mackay A L and Terrones H 1991 *Nature* **352** 762
[14] Terrones H, Terrones M and Moran-Lopez J L 2001 *Curr. Sci.* **81** 1011
[15] Terrones H, Terrones M and Hsu W K 1995 *Chem. Soc. Rev.* **24** 341
[16] Thurston W 1984 *Sci. Am.* **1** 108
[17] Kroto H W 1997 *Rev. Mod. Phys.* **69** 703–22
[18] Taylor R, Hare J P, Abdulsada A K and Kroto H W 1990 *J. Chem. Soc. Chem. Commun.* **20** 1423
[19] Fleming R M, Ramirez A P, Rosseinsky M J, Murphy D W, Haddon R C, Zahurak S M and Makhija A V 1991 *Nature* **352** 787
[20] Hebard A F, Rosseinsky M J, Haddon R C, Murphy D W, Glarum S H, Palstra T T M, Ramirez A P and Kortan A R 1991 *Nature* **350** 600
[21] Soto J R, Calles A and Moran-Lopez J L 2000 *J. Chem. Phys.* **113** 1055
[22] Dorset D L and Fryer J R 2001 *J. Phys. Chem.* B **105** 2356
[23] Kuzuo R, Terauchi M and Tanaka M 1994 *Phys. Rev.* B **49** 5054
[24] Fowler P W and Manolopoulos D E 1995 *Atlas of Fullerenes* (Oxford: Oxford University Press)
[25] Piskoti C, Yarger J and Zettl A 1998 *Nature* **393** 771
[26] Terrones M, Terrones G and Terrones H 2002 *Struct. Chem.* **13** 373
[27] Kikuchi K, Kobayashi K, Sueki K, Suzuki S, Nakahara H, Achiba Y, Tomura K and Katada M 1994 *J. Am. Chem. Soc.* **116** 9775
[28] Pasqualini E 1997 *Carbon* **35** 783
[29] Sijbesma R, Srdanov G, Wudl F, Castoro J A, Wilkins C, Friedman S H, Decamp D L and Kenyon G L 1993 *J. Am. Chem. Soc.* **115** 6510
[30] Friedman S H, Decamp D L, Sijbesma R P, Srdanov G, Wudl F and Kenyon G L 1993 *J. Am. Chem. Soc.* **115** 6506

[31] Heath J R, O'Brien S C, Curl R F, Kroto W H and Smalley R E 1987 *Comments Condens. Matter Phys.* **13** 119
[32] Von Helden G, Gotts N G and Bowers M T 1993 *Nature* **363** 60
[33] Hunter J, Fye J and Jarrold M F 1993 *Science* **260** 784
[34] Hernández E, Ordejón P and Terrones H 2001 *Phys. Rev.* B **63** 193403
[35] Iijima S 1980 *J. Cryst. Growth* **50** 675
[36] Brabec C J, Maiti A and Bernholc J 1994 *Chem. Phys. Lett.* **219** 473
[37] Maiti A, Brabec C J and Bernholc J 1993 *Phys. Rev. Lett.* **70** 3023
[38] Terrones M and Terrones H 1996 *Fullerene Sci. Technol.* **4** 517
[39] Terrones H and Terrones M 1997 *J. Phys. Chem. Solids* **58** 1789
[40] Heggie M I, Terrones M, Eggen B R, Jungnickel G, Jones R, Latham C D, Briddon P R and Terrones H 1998 *Phys. Rev.* B **57** 13339
[41] Jiao J, Seraphin S, Wang X K and Withers J C 1996 *J. Appl. Phys.* **80** 103
[42] Jiao J and Seraphin S 1998 *J. Appl. Phys.* **83** 2442
[43] Banhart F and Ajayan P M 1996 *Nature* **382** 433
[44] Hamada N, Sawada S and Oshiyama A 1992 *Phys. Rev. Lett.* **68** 1579
[45] Treacy M M J, Ebbesen T W and Gibson J M 1996 *Nature* **381** 678
[46] Ebbesen T W, Ajayan P M, Hiura H and Tanigaki K 1994 *Nature* **367** 519
[47] Terrones M *et al* 1997 *Nature* **388** 52
[48] Thess A *et al* 1996 *Science* **273** 483
[49] Hsu W K, Hare J P, Terrones M, Kroto H W, Walton D R M and Harris P J F 1995 *Nature* **377** 687
[50] Hsu W K, Terrones M, Hare J P, Terrones H, Kroto H W and Walton D R M 1996 *Chem. Phys. Lett.* **262** 161
[51] Iijima S 1993 *Mater. Sci. Eng.* B **19** 172
[52] Endo M, Takeuchi K, Igarashi S, Kobori K, Shiraishi M and Kroto H W 1993 *J. Phys. Chem. Solids* **54** 1841
[53] Bonard J M, Stora T, Salvetat J P, Maier F, Stockli T, Duschl C, Forro L, De Heer W A and Chatelain A 1997 *Adv. Mater.* **9** 827
[54] Duesberg G S, Burghard M, Muster J, Philipp G and Roth S 1998 *Chem. Commun.* **3** 435
[55] Bennemann K H, Reichardt D, Morán-López J L, Kerner R and Penson K 1994 *Z. Phys.* D **29** 231
[56] Dresselhaus M S, Dresselhaus G, Sugihara K, Spain I L and Goldberg H A 1988 *Graphite Fibers and Filaments* (*Springer Series in Materials Science* vol 5) (Berlin: Springer)
[57] Dresselhaus M S, Dresselhaus G and Eklund P C 1996 *Science of Fullerenes and Carbon Nanotubes* (San Diego, CA: Academic)
[58] Ajayan P M, Stephan O, Colliex C and Trauth D 1994 *Science* **265** 1212
[59] Guo T, Nikolaev P, Rinzler A G, Tománek D, Colbert D T and Smalley R E 1995 *J. Phys. Chem.* **99** 10694
[60] Terrones M 1997 Production and characterization of novel fullerene related materials: nanotubes, nanofibres and giant fullerenes *PhD Thesis* University of Sussex, UK
[61] Iijima S and Ichihashi T 1993 *Nature* **363** 603
[62] Ajayan P M, Lambert J M, Bernier P, Barbedette L, Colliex C and Planeix J M 1993 *Chem. Phys. Lett.* **215** 509
[63] Saito Y, Yoshikawa T, Okuda M, Ohkohchi M, Ando Y, Kasuya A and Nishina Y 1993 *Chem. Phys. Lett.* **209** 72
[64] Zhou D, Seraphin S and Wang S 1994 *Appl. Phys. Lett.* **65** 1593
[65] Journet C, Maser W K, Bernier P, Loiseau A, Delachapelle M L, Lefrant S, Deniard P, Lee R and Fischer J E 1997 *Nature* **388** 756
[66] Iijima S, Brabec C, Maiti A and Bernholc J 1996 *J. Chem. Phys.* **104** 2089
[67] Chopra N G, Benedict L X, Crespi V H, Cohen M L, Louie S G and Zettl A 1995 *Nature* **377** 135
[68] Ruoff R S and Lorents D C 1995 *Carbon* **33** 925
[69] Overney G, Zhong W and Tomanek D 1993 *Z. Phys.* D **27** 93
[70] Robertson D H, Brenner D W and Mintmire J W 1992 *Phys. Rev.* B **45** 12592

[71] Tersoff J 1992 *Phys. Rev.* B **46** 15546
[72] Wong E W, Sheehan P E and Lieber C M 1997 *Science* **277** 1971
[73] Langer L, Stockman L, Heremans J P, Bayot V, Olk C H, Vanhaesendonck C, Bruynseraede Y and Issi J P 1994 *J. Mater. Res.* **9** 927
[74] De Heer W A, Chatelain A and Ugarte D 1995 *Science* **270** 1179
[75] De Heer W A, Bacsa W S, Chatelain A, Gerfin T, Humphreybaker R and Forro L 1995 *Science* **268** 845
[76] Wildoer J W G, Venema L C, Rinzler A G, Smalley R E and Dekker C 1998 *Nature* **391** 59
[77] Wong E W, Sheehan P E and Lieber C M 1997 *Science* **277** 1971
[78] Schlittler R R, Seo J W, Gimzewski J K, Durkan C, Saifullah M S M and Welland M E 2001 *Science* **292** 1136
[79] Terrones M, Terrones H, Banhart F, Charlier J C and Ajayan P M 2000 *Science* **288** 1226–9
[80] Terrones M, Banhart F, Grobert N, Charlier J C, Terrones H and Ajayan P M 2002 *Phys. Rev. Lett.* **89** 075505
[81] Zunger A, Katzir A and Halperin A 1976 *Phys. Rev.* B **13** 5560
[82] Chopra N G, Luyken R J, Cherrey K, Crespi V H, Cohen M L, Louie S G and Zettl A 1995 *Science* **269** 966
[83] Terrones M, Hsu W K, Terrones H, Zhang J P, Ramos S, Hare J P, Castillo R, Prassides K, Cheetham A K, Kroto H W and Walton D R M 1996 *Chem. Phys. Lett.* **259** 568
[84] Terrones M, Benito A M, Mantecadiego C, Hsu W K, Osman O I, Hare J P, Reid D G, Terrones H, Cheetham A K, Prassides K, Kroto H W and Walton D R M 1996 *Chem. Phys. Lett.* **257** 576
[85] Loiseau A, Willaime F, Demoncy N, Hug G and Pascard H 1996 *Phys. Rev. Lett.* **76** 4737
[86] Fowler P W, Rogers K M, Seifert G, Terrones M and Terrones H 1999 *Chem. Phys. Lett.* **299** 359
[87] Blase X, Rubio A, Louie S G and Cohen M L 1994 *Europhys. Lett.* **28** 335
[88] Han W Q, Bando Y, Kurashima K and Sato T 1998 *Appl. Phys. Lett.* **73** 3085
[89] Golberg D, Bando Y, Kurashima K and Sato T 2000 *Solid State Commun.* **116** 1
[90] Lourie O R, Jones C R, Bartlett B M, Gibbons P C, Ruoff R S and Buhro W E 2000 *Chem. Mater.* **12** 1808
[91] Terauchi M, Tanaka M, Suzuki K, Ogino A and Kimura K 2000 *Chem. Phys. Lett.* **324** 359
[92] Shimizu Y, Moriyoshi Y, Tanaka H and Komatsu S 1999 *Appl. Phys. Lett.* **75** 929
[93] Cumings J and Zettl A 2000 *Chem. Phys. Lett.* **316** 211
[94] Chen Y, Chadderton L T, FitzGerald J and Williams J S 1999 *Appl. Phys. Lett.* **74** 2960
[95] Chen Y, Gerald J F, Williams J S and Bulcock S 1999 *Chem. Phys. Lett.* **299** 260
[96] Chopra N G and Zettl A 1998 *Solid State Commun.* **105** 297
[97] Hernández E, Gonze C, Bernier P and Rubio A 1998 *Phys. Rev. Lett.* **80** 4502
[98] Yakobson B I, Brabec C J and Bernholc J 1996 *Phys. Rev. Lett.* **76** 2511
[99] Terrones M, Grobert N and Terrones H 2001 *Carbon* **40** 1665
[100] Terrones M *et al* 1999 *Adv. Mater.* **11** 655
[101] Terrones M *et al* 1999 *Appl. Phys. Lett.* **75** 3932
[102] Blase X, Charlier J C, De Vita A, Car R, Redlich Ph, Terrones M, Hsu W K, Terrones H, Carrol D L and Ajayan P M 1999 *Phys. Rev. Lett.* **83** 5078
[103] Czerw R *et al* 2001 *Nanoletters* **1** 457
[104] Tenne R, Margulis L, Genut M and Hodes G 1992 *Nature* **360** 444
[105] Mar-gulis L, Salitra G, Tenne R and Talianker M 1993 *Nature* **365** 113
[106] Tenne R, Homyonfer M and Feldman Y 1998 *Chem. Mater.* **10** 3225
[107] Rapoport L, Bilik Y, Feldman Y, Momyonfer M, Cohen S R and Tenne R 1997 *Nature* **387** 791
[108] Seifert G, Terrones H, Terrones M, Jungnickel G and Frauenheim T 2000 *Solid State Commun.* **114** 245
[109] Seifert G, Terrones H, Terrones M, Jungnickel G and Frauenheim T 2000 *Phys. Rev. Lett.* **85** 146
[110] Nath M and Rao C N R 2001 *J. Am. Chem. Soc.* **123** 4841
[111] Seifert G, Terrones H, Terrones M and Frauenheim T 2000 *Solid State Commun.* **115** 635
[112] Coleman K S, Sloan J, Hanson N A, Brown G, Clancy G, Terrones M, Terrones H and Green M L H 2002 *J. Am. Chem. Soc.* **124** 11580
[113] Brorson M, Hansen T W and Jacobsen C J A 2002 *J. Am. Chem. Soc.* **124** 11582

[114] Subramoney S, Kavelaee V, Ruoff R S, Lorents D C, Malhotra R and Kazmer A J 1994 *Chemistry and Physics of Fullerenes and Related Materials* (Pennington, NJ: The Electrochemical Society) p 1498
[115] Liu M Q and Cowley J M 1995 *Carbon* **33** 225
[116] Subramoney S, Ruoff R S, Lorents D C, Ethan B, Malhotra R, Dyer M J and Parvin K 1994 *Carbon* **32** 507
[117] Loiseau A and Pascard H 1996 *Chem. Phys. Lett.* **256** 246
[118] Tsang S C, Chen Y K, Harris P J F and Green M L H 1994 *Nature* **372** 159
[119] Chen Y K, Green M L H and Tsang S C 1996 *Chem. Commun.* **21** 2489
[120] Sloan J, Cook J, Heesom J R, Green M L H and Hutchison J L 1997 *J. Cryst. Growth* **173** 81
[121] Sloan J, Cook J, Green M L H, Hutchison J L and Tenne R 1997 *J. Mater. Chem.* **7** 1089
[122] Chen Y K, Chu A, Cook J, Green M L H, Harris P J F, Heesom R, Humphries M, Sloan J, Tsang S C and Turner J F E 1997 *J. Mater. Chem.* **7** 545
[123] Tsang S C, Davis J J, Green M L H, Allen H, Hill O, Leung Y C and Sadler P J 1995 *J. Chem. Soc. Chem. Commun.* **17** 1803
[124] Tsang S C, Guo Z J, Chen Y K, Green M L H, Hill H A O, Hambley T W and Sadler P J 1997 *Angew. Chem. Int. Edn Engl.* **36** 2198
[125] Ajayan P M and Iijima S 1993 *Nature* **361** 333
[126] Ajayan P M, Ebbesen T W, Ichihashi T, Iijima S, Tanigaki K and Hiura H 1993 *Nature* **362** 522
[127] Dujardin E, Ebbesen T W, Hiura H and Tanigaki K 1994 *Science* **265** 1850
[128] Grobert N *et al* 1999 *Appl. Phys. Lett.* **75** 3363
[129] Grobert N *et al* 2001 *Chem. Commun.* **5** 471
[130] Hsu W K, Terrones M, Terrones H, Grobert N, Kirkland A I, Hare J P, Prassides K, Townsend P D, Kroto H W and Walton D R M 1998 *Chem. Phys. Lett.* **284** 177
[131] Terrones H 1994 *J. Math. Chem.* **15** 143
[132] Balaban A T, Klein D J and Liu X 1994 *Carbon* **32** 357
[133] Ge M and Sattler K 1994 *Chem. Phys. Lett.* **220** 192
[134] Krishnan A, Dujardin E, Treacy M M J, Hugdahl J, Lynum S and Ebbesen T W 1997 *Nature* **388** 451
[135] Ijima S, Yudasaka M, Yamada R, Bandow S, Suenaga K, Kokai F and Takahashi K 1999 *Chem. Phys. Lett.* **309** 165
[136] Bourgeois L, Bando Y, Han W Q and Sato T 2000 *Phys. Rev.* B **61** 7686
[137] Terrones H *et al* 2001 *Chem. Phys. Lett.* **343** 241
[138] Charlier J C and Rignanese G M 2001 *Phys. Rev. Lett.* **86** 5970
[139] Lenosky T, Gonze X, Teter M and Elser V 1992 *Nature* **355** 333
[140] Vanderbilt D and Tersoff J 1992 *Phys. Rev. Lett.* **68** 511
[141] Okeeffe M, Adams G B and Sankey O F 1992 *Phys. Rev. Lett.* **68** 2325
[142] Terrones H, Fayos J and Aragon J L 1994 *Acta Metall. Mater.* **42** 2687
[143] Terrones H and Mackay A L 1993 *Chem. Phys. Lett.* **207** 45
[144] Terrones H and Terrones M 1997 *Phys. Rev.* B **55** 9969
[145] Itoh S, Ihara S and Kitakami J 1993 *Phys. Rev.* B **47** 1703
[146] Ihara S, Itoh S and Kitakami J 1993 *Phys. Rev.* B **47** 12908
[147] Amelinckx S, Zhang X B, Bernaerts D, Zhang X F, Ivanov V and Nagy J B 1994 *Science* **265** 635
[148] Ricardo-Chávez J L, Dorantes-Dávila J, Terrones M and Terrones H 1997 *Phys. Rev.* B **56** 12143
[149] Terrones H, Terrones M, Hernández E, Grobert N, Charlier J C and Ajayan P M 2000 *Phys. Rev. Lett.* **84** 1716
[150] *Report on the Scientific Results of the Voyage of the HMS Challenger During the Years 1873–1876, Zoology* 1887 vol 18 (London: Her Majesty's Stationery Office)